The Meisenheimer Complex as a Paradigm in Drug Discovery: Reversible Covalent Inhibition through C67 of the ATP Binding Site of PLK1

Russell J. Pearson,[1,4] David G. Blake,[2] Mokdad Mezna,[2] Peter M. Fischer,[3] Nicholas J. Westwood,[4] and Campbell McInnes[2,5,6,*]

[1]School of Pharmacy, Keele University, Staffordshire ST5 5BG, UK

[2]Cyclacel Ltd., James Lindsay Place, Dundee DD1 5JJ, UK

[3]School of Pharmacy and Centre for Biomolecular Sciences, University of Nottingham, NG7 2RD, UK

[4]Department of Chemistry, University of St Andrews, Fife KY16 9ST, UK

[5]Drug Discovery and Biomedical Sciences, University of South Carolina, Columbia, SC 29208, USA

[6]Lead Contact

*Correspondence: mcinnes@cop.sc.edu

SUMMARY

The polo kinase family are important oncology targets that act in regulating entry into and progression through mitosis. Structure-guided discovery of a new class of inhibitors of Polo-like kinase 1 (PLK1) catalytic activity that interact with Cys67 of the ATP binding site is described. Compounds containing the benzothiazole N-oxide scaffold not only bind covalently to this residue, but are reversible inhibitors through the formation of Meisenheimer complexes. This mechanism of kinase inhibition results in compounds that can target PLK1 with high selectivity, while avoiding issues with irreversible covalent binding and interaction with other thiol-containing molecules in the cell. Due to renewed interest in covalent drugs and the plethora of potential drug targets, these represent prototypes for the design of kinase inhibitory compounds that achieve high specificity through covalent

interaction and yet still bind reversibly to the ATP cleft, a strategy that could be applied to avoid issues with conventional covalent binders.

INTRODUCTION

The Polo-like kinases (PLKs) are serine/threonine protein kinases that are key regulators of the cell cycle, and in mammals have been reported to play numerous roles in regulating entry into and progression through mitosis (Craig et al., 2014; McInnes and Wyatt, 2011). PLK1 is expressed throughout the cell cycle, although its activity peaks late in G2 and is sustained through mitosis (Hamanaka et al., 1995; Lee et al., 1995). At the end of G2, through phosphorylation and promotion of nuclear translocation (Toyoshima-Morimoto et al., 2002), PLK1 acts on CDC25C (Roshak et al., 2000), resulting in activation of CDK1/cyclin B by removal of inhibitory phosphate groups (Nurse, 1990). PLK1 also promotes sister chromatid separation mediated by activation of the APC (Golan et al., 2002; Kotani et al., 1998), and also through phosphorylation of the SCC1 subunit of cohesin (Alexandru et al., 2001; Sumara et al., 2004). Mitotic exit occurs after PLK1 interacts with and phosphorylates the kinesin-like protein, CHO1/MKLP-1 and promotes cytokinesis (Lee et al., 1995). Four closely related PLKs exist in humans (Glover et al., 1998) and structurally contain two separate, highly homologous domains: an amino-terminal region that contains the catalytic kinase domain and a C-terminal domain that has two conserved Polo-box regions (Elia et al., 2003a, 2003b) (one in PLK4 [Leung et al., 2002]). A fifth PLK has been identified but shown to lack a kinase domain (de Carcer et al., 2011). The polo boxes function in recruitment for subcellular localization and compartmentalization (Lee et al., 1998). Furthermore there is evidence suggesting that the Polo-box domain (PBD) participates in regulating interactions with substrates, e.g., CDC25C phosphatase (Elia et al., 2003a, 2003b), as an autoregulatory domain (Jang et al., 2002). Furthermore, PBD-dependent PLK1 activity is required for proper metaphase/anaphase transition and cytokinesis (Seong et al., 2002; Yuan et al., 2011).

Overexpression of PLK1 is a common occurrence in cancer and is of prognostic value for several tumor types (Knecht et al., 1999; Takahashi et al., 2003; Tokumitsu et al., 1999; Wolf et al., 1997; Yuan et al., 1997). In addition, constitutive expression of PLK1 in mammalian cells can lead to malignant transformation (Smith et al., 1997). PLK1 has been extensively validated as an anti-tumor drug target using a variety of cellular and in vivo studies. Downregulation of PLK1 activity, through the administration of antisense oligonucleotides

and small interfering RNA molecules, has been demonstrated to be highly effective in inhibition of proliferation of cancer cells both in vitro and in vivo (Elez et al., 2000, 2003; Spankuch-Schmitt et al., 2002a, 2002b). Several drug candidates have been investigated in human trials including BI2536 and GSK461364A, with the most advanced compound being volasertib (BI-6727), shown to have clinical efficacy in combination with cytarabine in acute myeloid leukemia (Dohner et al., 2014; Gjertsen and Schoffski, 2014). Although promising activity has been observed, there is continued scope to improve clinical outcomes through optimization of mechanism of inhibition and pharmacokinetic and dynamic properties.

Here a structure-guided design approach to the discovery and development of benzothiazole *N*-oxide PLK1 inhibitors is described. These highly selective molecules inhibit the enzyme through a covalent but reversible mechanism involving a Meisenheimer complex (MC), which is without precedent in the protein kinase literature. In recent years, covalent inhibition of drug targets, and especially of protein kinases, has been recognized as an effective approach to improving selectivity and for overcoming drug resistance; however, this is not without significant issues including potential toxicities (Baillie, 2016). Inhibition through MC formation is a promising strategy to combine the benefits of a covalent mechanism while retaining reversible binding to the drug target of interest. A recent report described the observation of a MC in the context of nitrobenzothiazinone anti-tuberculosis drugs; however, it did not elaborate these as contributing to potency and selectivity but merely from the standpoint of the metabolic implications for continuing development of this important class of drugs (Kloss et al., 2017). The compounds described herein therefore represent prototypes and proof of concept for exploiting the MC in kinase inhibition and potentially more broadly in drug discovery.

RESULTS

PLK1 Is Irreversibly and Selectively Inhibited by Thiol Modifying Agents

A structure-guided approach for the discovery of the cyclapolin benzothiazole *N*-oxide class of inhibitors has been described (McInnes et al., 2006). This approach preceded the determination of the crystal structure of PLK1 kinase domain. Upon construction of a homology structure and examination of the ATP binding site residues, it was observed that PLK1 had some unusual features compared with other protein kinases. In particular, the residue at the end of the glycine-rich loop that commonly interacts with the ribose of ATP,

and is frequently a valine, occurs as a cysteine in PLK1 (C^{67}). This residue in other protein kinase-ligand crystal structures generally makes significant contacts with ATP competitive small molecules (e.g., V^{18} in CDK2). The unique characteristic of C^{67} in PLK1 thus could allow exploitation of the nucleophilicity of the thiol side chain to enable covalent binding of PLK1 inhibitors.

The development of irreversible kinase inhibitors has precedent in the literature in the context of the epidermal growth factor receptor tyrosine kinases, where non-covalently binding ATP competitive compounds were converted by addition of a geometrically appropriate reactive functionality (Singh et al., 1997). These compounds were designed to form a covalent bond with a cysteine in the kinase active site and thus to take advantage of the thiol attack on the inhibitor. In the erbB1 kinase domain, 2'-thioadenosine (2TA), **1** (Figure 1), places the thiol adjacent to the C^{833} and was shown in this to form a disulfide bond and to inhibit the kinase activity. As the active site cysteine (C^{67}) is on the opposite face of the ATP cleft in the PLK1 context, inhibition would necessitate the synthesis of 5'-thioadenosine (5TA), **2**, (Figure 1) so as to position the ribose thiol proximal to the reactive side chain. Flexible docking of 5TA **2**, with PLK1 was completed and the binding mode was verified through comparison with ATP bound crystal structures. Further to this, the disulfide link between C^{67} and 5TA **2**, was formed in silico and resulted in a conformation (Figure 2) similar to the experimental binding mode observed in other kinases. Subsequent to this, **2** was synthesized and shown to inhibit PLK1 kinase activity with a half maximal inhibitory concentration (IC_{50}) of 39 μM. 2TA **1**, exhibited markedly lower inhibition (120 μM) and adenosine **3** (Figure 1), itself had no observed activity against PLK1 (>200 μM).

Discovery of Potent and Selective Inhibitors of PLK1 Using Lidaeus

The homology model of the kinase domain of PLK1 was validated through the observed correlation of intermolecular contacts and binding energies of known inhibitors and through the assay results obtained from the use of thiol-modifying agents. Since it was considered to be of sufficient computational reliability, the model structure was further used in high-throughput docking calculations to identify novel PLK1 starting points. To carry out this task, one of the previously docked thiazole anilino-pyrimidine compounds in complex with PLK1 was used as a template structure for Lidaeus calculations. Lidaeus (Taylor et al., 2008; Wu et al., 2003), a tool for rapid flexible docking of ligands into protein binding sites, generates site

points from energies of probe atoms within a specified radius of the inhibitor. Interatomic ligand vectors are then matched with the site points from fragments of the molecule followed by positioning of subsequent fragments and ranking by overall intermolecular energy score. As previously described, using the complex of a pyrimidine derivative with PLK1, Lidaeus was employed to dock approximately 200,000 commercially available small molecules. From these, 350 *in-silico*-ranked compounds were assayed for PLK1 inhibition in a radiometric kinase assay quantifying the amount of radiolabeled ATP incorporated into the CDC25C substrate. A number of *in vitro* PLK1 inhibitors emerged from this strategy with an overall hit rate of 1% and a potency range of 0.5–20 μM IC_{50}. While several confirmed hits were obtained, one series had more potent activity in the kinase assay and consisted of a benzothiazole *N*-oxide core structure. The obtained hit, **4** (Table 1), was promising not only from its micromolar potency but also from its low molecular weight and potential for synthesizing a number of derivatives that could optimize potency and drug-like properties. The phenotypic activity of compound 4 has previously been described where novel roles of PLK1 in spindle pole maintenance were demonstrated through use of this molecule as a chemical biology probe (McInnes et al., 2006). The structure-activity relationship of **4** and its related analogs are described for the first time in the following results.

Structure-Activity Relationship Determination of Benzothiazole Inhibitors

Subsequent to the identification of **4** as a potent PLK1 inhibitor, a set of commercial compounds expanding on the benzothiazole *N*-oxide scaffold were obtained and tested for inhibition of PLK1. This included a significant number of secondary amide and ester derivatives at the R_3 position of the thiazole ring. Surprisingly none of these compounds exhibited any significant level of *in vitro* inhibition of PLK1, thus suggesting an important contribution of the primary amide (see structure in Table 1, inactive esters not shown) to binding.

To further explore the structure-activity relationship (SAR) of this series, a synthetic route for the benzothiazole *N*-oxide was developed, and a number of analogs related to the *in silico* hit compound were prepared. Firstly, the substituents on the aryl component of the pharmacophore were modified, and testing of these compounds in the PLK1 assay yielded information on the SAR. A number of derivatives were synthesized (Table 1) replacing the CF_3 with other groups and included fluoro **5**, iodo **6**, methyl ester **7**, nitrile **8**, and methyl **9**.

Surprisingly, only compounds possessing electron-withdrawing substituents in this position exhibited activity against PLK1. In particular, the methyl group derivative **9**, which is isosteric with CF_3, was completely inactive. When the CF_3 group in the *in-silico*-discovered compound was replaced with a trifluoromethyl-thioether **10**, an increase in potency was observed. This compound increased in potency from 2.5 to approximately 0.4 μM, suggesting that the spacing functionality resulted in more complementary interactions of the CF_3 group in the ATP binding site. Generation of the free carboxylate group from hydrolysis of the methyl ester **7**, to generate compound **11**, interestingly resulted in an inactive molecule.

Further synthetic modification of the substituents on the thiazole ring were carried out and revealed that the incorporation of other small polar groups replacing the amide resulted in active compounds, although none as potent as the parent hit (Table 1). Compounds tested included those with nitrile **12**, hydroxamate **13**, and hydrazide **16** functions.

An additional observation made was that closely related compounds lacking the *N*-oxide on the thiazole ring were completely devoid of activity as exemplified by the reduction of the *N*-oxide in **4** to generate **14** and that of the reduction of **10** to its counterpart (data not shown). These results were not in line with the predicted small contribution of a single atom to intermolecular binding but pointed to the importance of the electrostatic nature and electron-withdrawing potential of the *N*-oxide functionality. Further SAR for the benzothiazole *N*-oxide series was established through the synthesis of compound **15** with the CF_3 and nitro groups reversed. This compound was surprisingly inactive pointing to essential interactions of the nitro group with the ATP binding site of PLK1.

To gain some insight into the binding of the benzothiazole *N*-oxide lead compounds in the PLK1 ATP cleft, and to assess the contributions of various substituents for binding, molecular docking experiments were carried out using the PLK1 model structure and subsequently with the available crystal structures. Using this approach, numerous docking solutions were evaluated in terms of interaction energy, docking score, and, with respect to consistency, with known kinase inhibitory interactions. Particular attention was paid to the observed requirement for a primary amide group on the thiazole. A binding mode that fulfilled each of these criteria was observed (Figure 3). Interestingly, C^{67} is in close proximity to the C4 (aromatic ring) of the benzothiazole system, although it does not make the complementarity expected from the valine residue that is commonly found in this position. In addition, the interactions observed in the docked structure provided a clear rationale for CF_3S group. These calculations indicate that the CF_3S projects into a subpocket and shows a high

degree of complementarity with this region. A good correlation was observed between the non-bonded docking score and the potency of the inhibitors.

Benzothiazole *N*-Oxide Inhibitors Interact Covalently with the PLK1 Active Site

To confirm that the benzothiazoles were binding to the ATP cleft of PLK1 and were not targeting substrate binding or possibly another site resulting in allosteric inhibition of ATP binding, the $K_{m,ATP}$ was determined at various inhibitor concentrations. This measurement was repeated for two of the most potent PLK1 inhibitory compounds, **4** and **10**. While compound 4 (2.5 μM IC_{50}) was shown to be ATP competitive, as demonstrated by the variation in the K_m for ATP, the significantly more potent analog, **10** was found to have similar K_m for ATP at every ligand concentration studied (Figure 4). These data indicate that the equilibrium of binding for compound **10** shifts toward being non-ATP competitive in contrast to inhibitor **4**. In light of these results, observation of the C^{67} side chain in the PLK1 model structure and the outcomes of using thiol modifying agents, it was hypothesized that these compounds may be interacting covalently with the cysteine. Further investigation into the chemistry of the benzothiazole *N*-oxide series suggested a literature precedent for reactivity and susceptibility to nucleophilic attack on the aromatic ring (Bunting, 1979). This reaction has been shown to occur ortho or para to a nitro-substituted phenyl ring, where a covalent intermediate is formed as per the mechanism shown above Table 2, and has been named the ‘‘Meisenheimer complex.’’

Examination of the docked structure of **4** with the PLK1 model structure indicates a close proximity of the thiol of C^{67} and the C4 aromatic carbon (para to the nitro group and highlighted in Figure 3), and hence strongly supports this hypothesis. Confirmation of the MC was indicated through a set of model ^1H nuclear magnetic resonance (NMR) experiments with the active and inactive compounds from the benzothiazole series. Addition of *n*-butylamine as a surrogate nucleophile to the active compounds including **4**, **7**, **8**, and **10**, in each case, resulted in a dramatic color change of the compound in solution. For solubility purposes, all of these experiments relied on the use of the ethyl ester derivatives of each benzothiazole ($R_3 = CO_2Et$) dissolved in deuterated chloroform, and therefore the majority of model reactions were carried out using *n*-butylamine. Experiments were also undertaken with sodium 1-butanethiolate and showed similar dramatic changes in the color of the compound solution and in the UV spectrum (Figures S1 and S2). The requirement for polar aprotic

NMR solvents (potentially reactive) to solubilize the 1-butanethiolate precluded NMR experiments with this more appropriate model nucleophile. On the other hand, non-polar solvents did not allow NMR study of the MC due to a lack of compound solubility.

Further experiments utilizing UV-vis spectrophotometry were carried out to support this hypothesis using ethanol as the solvent of choice. During initial experiments to identify the presence of the MC, it was observed that highly colored solutions were obtained upon addition of the model nucleophile (*n*-butylamine) to the benzothiazole *N*-oxide inhibitor, an observation consistent with the literature, where a red shift in the UV-vis spectrum is seen for λ_{max} (Taylor, 1970). An extensive UV-vis spectrophotometric characterization of the series of active and inactive benzothiazoles was subsequently carried out to examine if a relationship existed between the induced color change and potency of the pharmacophoric series (Table 2). It was determined that, for each of the active PLK1 inhibitors from this series, a substantial shift in UV absorbance was identified, accompanied by a dramatic increase in extinction coefficient for the new signal. Out of eight compounds tested, all six analogs with measurable IC_{50} values against PLK1 exhibited a significant UV shift and an enhancement of extent of absorbance. Conversely, neither of the inactive molecules in the series displayed either a UV shift or an increase in extinction coefficient (**9a** and **11a**). In addition, a rough correlation of the increase in absorbance and potency of the compounds can be extracted from the measured data. Furthermore two additional inactive compounds in this series were tested and no UV shift or absorbance increase was observed (data not shown).

Further characterization of the ^{1}H NMR spectra of the inhibitors before and after addition of the nucleophile (*n*-butylamine) resulted in a disappearance of both the aromatic protons in the spectrum (Table 2) and a shift of the signals further upfield, which is characteristic of the cyclohexa-2,5-dien-1-ylidene azinate structure formed after nucleophilic attack (see above Table 2). Subsequent examination of the inactive compounds in a similar experimental protocol determined that for these benzothiazoles, no change in the aromatic ^{1}H NMR signals occurred. This was shown to be true for the previous incongruously inactive compounds, including the CF_3 to CH_3 replacement, **9**, and the carboxylate derivative, **11**. Analysis of the compounds (those active against PLK1) recovered after removal of the *n*-butylamine showed that there was no evidence of the Meisenheimer adduct therefore confirming that this is a fully reversible reaction.

Activity of Compound 4 and volasertib (BI6727) against PLK1 WT and PLK1 C67S

To confirm whether C^{67} plays a role in the activity of the benzothiazole *N*-oxide series, as strongly suggested by the SAR data, along with the enzyme kinetics and spectroscopy results, compound **4** was investigated along with volasertib (BI6727), a potent PLK1 ATP inhibitor currently approved by the US Food and Drug Administration for the treatment of acute myeloid leukemia. Due to requirements for commercial assay screening, these compounds were tested against the wild-type PLK1 with a lower ATP concentration than previously used and shown to have IC_{50} values of 0.463 and 0.016 μM, respectively. Subsequent to this, a mutant PLK1 enzyme possessing the exchange of cysteine 67 for serine, was generated. As serine is considerably less nucleophilic than the native cysteine residue, it would not be expected to form the MC to a significant degree and therefore the activity of the benzothiazole *N*-oxide series should be dramatically lower in the context of this mutant. Testing of volasertib in the first instance showed that while its activity against PLK1 C67S was reduced compared with the wild-type, an IC_{50} of 0.151 μM was obtained (Figure 5). Staurosporine was also shown to potently inhibit PLK1 C67S (Figure S3). This contrasted to compound **4**, which was found to be completely inactive at concentrations of >100 μM, thereby providing confirmation that Cys^{67} forms a covalent MC with the benzothiazole *N*-oxide series as strongly suggested by the previously described data.

Kinase Selectivity and Cellular Activity of Lead Inhibitors

Since specificity can be problematic in the development of ATP competitive inhibitors of any protein kinase, the benzothiazole *N*-oxide series was tested on a panel of in-house enzymes (Table S1). Interestingly none of these were inhibited by the *in-silico*-identified lead compound **4**. To further probe the selectivity of this compound, a further 20 kinases available from an out-sourced screen were examined for inhibition in the presence of 100 μM of **4**, and included three kinases with a cysteine in the position equivalent to PLK1 (Table S2). None of this additional panel exhibited a significant level of inhibition, with the exception of CSK, whose activity was slightly blocked by the action of this compound (<50% inhibition at 100 μM compound). Due to the level of potency obtained for this fragment like series, and the high degree of selectivity observed, it is apparent that the specificity arises from the demonstrated mechanism of inhibition through the MC. The selectivity of the most potent

inhibitor, **10**, was also examined by testing against an in-house kinase panel and confirmed its selectivity toward PLK1.

DISCUSSION

The results presented here demonstrate that an approach to generating PLK1 inhibitors involving homology modeling, molecular docking of known ligands, and *in vitro* testing has determined novel features of the PLK1 ATP binding site that can be exploited in the structure-guided design of compounds specific for this kinase. The ability to selectively inhibit PLK1 via covalent interaction with C^{67} of the ATP binding site was confirmed through the synthesis of thio-adenosine derivatives (**1** and **2**). The cysteine is located on the glycine-rich loop in the *N*-lobe region in the position occupied by a valine in the majority of protein kinases and is quite unique to the PLKs. The preferential inhibition of PLK1 by 5TA, **2**, which, according to known kinase-ATP structures and subsequent modeling (Figure 2) in the PLK1 context, results from proximity of the thiol group to the reactive cysteine (as opposed to the 2'-thio derivative, where the thiol group projects toward the C-lobe and therefore would be less able to react with C^{67}). Although 2TA, **1**, inhibits PLK1 to a certain degree, its observed activity probably results from the flexibility of the ribose in the ATP binding site, enabling reaction with the cysteine residue. In addition, the observation that adenosine does not inhibit PLK1 gives weight to the hypothesis that selective covalently interacting inhibitors can be designed and synthesized based on the structural information obtained from this approach. These results, taken as a whole, strongly suggest that the cysteine residue present in the PLK1 ATP cleft can form covalent interactions with appropriately positioned electrophilic groups in an inhibitor. This novel feature of PLK1 should thus enable the discovery and design of inhibitors that potently and selectively inhibit the activity of PLKs. To this end, as the homology structure was extensively validated, it was confidently utilized for database searching for new PLK1 inhibitors and resulted in the identification of the benzothiazole *N*-oxide pharmacophore. Results show that potency and selectivity for PLK1 over many other kinases can be achieved through this chemical series, which not only binds avidly to the active site but also interacts covalently with C^{67}. While the homology structure was used in initial studies to propose the covalent mechanism of inhibition and for discovery of the benzothiazole *N*-oxide inhibitors, the publication of multiple crystal structures of the PLK1 kinase domain confirmed the position of C^{67} and further validated the results obtained with the homology structure. Furthermore, compounds

were redocked with PLK1 crystal structures and, as expected, also found to have binding modes compatible with formation of the MC.

It is apparent from these results that the necessity for an electron-withdrawing group on the phenyl substituent of the benzothiazole, and the presence of the *N*-oxide for PLK1 inhibition, relate to the ability of these compounds to form MCs. This was determined by demonstrating a correlation between inhibitors of the benzothiazole series that show activity against PLK1 and their ability to induce spectroscopic changes upon addition of a model nucleophile. This was further supported by the requirement of the R_1 position (see Table 1) to be an electron-withdrawing substituent. Small changes in the chemical structure of this series (i.e., replacement with isosteric groups, e.g., CF_3 to CH_3 or removal of the *N*-oxide functionality), which should not be so detrimental to kinase activity, resulted in complete lack of PLK1 inhibition. These changes do not significantly alter the steric nature of the inhibitor, but would dramatically change the electronic nature of the structures. Increasing the electron-withdrawing character at R_1 would therefore make the C4 and C6 positions of the nitro-substituted benzothiazole ring less electron-rich and more susceptible to nucleophilic attack, resulting in formation of the MC (see above Table 2). This was corroborated by the observed correlations that exist between the electronegativity of the R_1 and R_2 groups and the inhibitor potency, and also between the UV absorbance of the Meisenheimer adduct and the PLK1 activity.

The higher potency of compound **10** and the differing kinetics versus **4** (Figure 4.) can be explained by the greater affinity and complementarity of the SCF_3 group with the PLK1 ATP binding site and the structural basis for this potency increase has been determined computationally. The SCF_3 group has almost twice the lipophilicity of the CF_3 group and therefore has greater potential to interact through van der Waals interactions in a binding pocket (Feng et al., 2016). Calculations show that the SCF_3 of **10** has a significantly higher degree of complementarity with a sub-pocket of the ATP binding site compared with CF_3 (**4**), occupying it almost completely and therefore explaining the potency increase in these terms alone (the significantly increased interactions of the SCF_3 group are shown comparatively; Figure S4). As a result and consistent with enzyme inhibition kinetics, it is known that, if the affinity is tight enough, compounds can display non-competitive behavior. The kinetic differences of **4** versus **10** can be explained by the increased potency of **10**, which results in stabilization of the binding mode and therefore, by extension, the covalent MC (Table 1). Other explanations such as displacement of the SCF_3 group or differences in the oxidation of

the two compounds are very unlikely due to the similar electronegativities of the CF_3 and SCF_3 groups, and also the restrictions on the nucleophilic aromatic substitution reaction (SNAr) in this system.

The lack of inhibition of the carboxylate derivative **11**, despite possessing an electron-withdrawing substituent most probably results from delocalization of the negative charge into the aromatic ring thus disfavoring nucleophilic attack. This was supported by the observation that this compound was refractory to formation of the MC, as demonstrated by the described spectroscopic methods. Reversal of the CF_3 and NO_2 groups of **4** to generate compound **15** resulted in complete loss of activity on PLK1, an effect probably due to the critical nature of the nitro function to direct binding, and supported by electrostatic interactions with K^{82} in the docked structures (Figure 3). Since the nitro group is acting as an electron sink it will be more negatively charged in the MC and therefore contributes significantly to the enthalpy of binding.

Confirmation for the MC formation and the resulting covalent inhibition of PLK1 through C^{67} was obtained through comparison of the activities of compound **4** and volasertib (BI6727) in inhibiting the wild-type PLK1 versus the C67S mutant. The retention of potent activity of volasertib for the mutant PLK1 and the complete loss of inhibition of **4** in this context provides strong evidence that the benzothiazole *N*-oxide series act through MC formation. The decreased activity of volasertib with PLK1 C67S is most likely due to the loss of van der Waals contacts in the context of the serine as the oxygen has a significantly smaller atomic radius than the sulfur.

The formation of the Meisenheimer adduct between the benzothiazole ring and the sulfur nucleophile leads to high-affinity binding of this series and is likely responsible for the selectivity for PLK1 versus all of the other enzymes tested. This method of kinase inhibition is currently without precedent in the literature, and has been demonstrated to be a paradigm through which selective kinase inhibitors can be obtained. Despite the observation that these act through covalent bond formation with the reactive cysteine in the PLK1 active site, this series should not suffer from reactivity with general nucleophilic groups in biological milieu since the MC is not a stable intermediate and is under normal conditions fully reversible. This was demonstrated in the context of the benzothiazole *N*-oxide series in that no stable intermediate MC could be isolated after addition of model nucleophiles even though the presence of this species was confirmed using two spectroscopic methods.

In addition to the experimental methods used and which confirmed the mechanism of inhibition of the benzothiazole series through the MC, the molecular docking calculations that were carried out strongly support the proposed covalent interaction with C^{67}. The binding modes and interaction energetics generated using a rigorous molecular mechanics docking approach (allowing flexibility of both the ligand and ATP binding site residues) were predicted for a set of the active analogs. As the SAR data pointed to the critical nature of the primary amide group, and since a frequent binding determinant of kinase inhibitors includes an H-bond donor and acceptor pair to the interdomain connecting loop (‘‘hinge’’), it is highly probable that the amide is responsible for these interactions (no other H-bond donors in the parent benzothiazole molecule, **4**). Docking of other active isosteres at this position including the nitrile **12**, hydroxamate **13**, and the hydrazide **16** derivatives confirm the contributions of the hinge contacts, and therefore the overall binding mode. Overall, an excellent correlation between the interaction energy of this series of benzothiazole N-oxide derivatives and the IC_{50} values was observed and therefore confirms the binding mode that positions C^{67} for nucleophilic attack to form the MC.

A study has demonstrated that potent and selective inhibitors of protein kinases could be obtained using a structural bioinformatics approach that targeted the corresponding cysteine described in this work as resulting in specific PLK1 inhibition (Cohen et al., 2005). Sequence alignment analysis revealed that eight other protein kinases have the equivalent cysteine residue representing four different kinase families. In this example, however, in addition to cysteine, a threonine ‘‘gatekeeper’’ was required in order to provide additional space for a substituent on the designed inhibitor. While three of these kinases (MSK2, NEK2, and RSK1) were probed for inhibition by compounds **4** and **10**, and no significant activity observed, each could potentially be inhibited by appropriate tuning of the inhibitor containing a ‘‘Meisenheimer Complex Scaffold.’’ Furthermore, recent work described the analysis of cysteine residues across the human kinome and which would be available for covalent inhibitor development (Zhao et al., 2017). This study concluded that there are 44 kinases containing cysteine residues that have been successfully exploited by covalent kinase inhibitors. There is, therefore, a plethora of potential kinase drug targets that the MC approach could be applied to for potent and selective inhibition. While resistance through mutation of the cysteine residue is always possible, it remains so regardless of the mode of covalent inhibition.

In summary, through study of the PLK1 kinase domain, unique features of its ATP binding site have been exploited in the discovery and design of inhibitors. A class of PLK1 inhibitors based on the benzothiazole N-oxide have been described and shown to selectively inhibit the enzyme through an MC, a mechanism of action not previously described for protein kinase inhibitors. This pharmacophore represents a prototype for a new approach to generate PLK1 inhibitors and, in fact, inhibitors in general that possess high selectivity through reversible covalent interaction. Such inhibitors have the potential added benefit of minimizing off target effects that occur with irreversible inhibitors.

SIGNIFICANCE

The Polo family of mitotic kinases are clinically validated oncology targets. Structure-based discovery and design has led to a class of inhibitors of PLK1 catalytic activity that covalently interact with C^{67} of the ATP binding site. Benzothiazole *N*-oxide derivatives reversibly inhibit PLK1 through the formation of Meisenheimer complexes, a mechanism of kinase inhibition, which yields high selectivity while avoiding off target effects that occur through covalent binding to other thiol-containing molecules in the cell. Due to recent renewed interest in covalently binding inhibitors as a class of drugs, and the plethora of targets that can be inhibited using this approach, these compounds represent prototypes for the design of kinase inhibitors and, in fact, inhibitors in general that exploit the Meisenheimer complex to generate potent and selective compounds that potentially also avoid toxicity issues arising for irreversibly binding drugs.

STAR METHODS

Detailed methods are provided in the online version of this paper and include the following:

- KEY RESOURCES TABLE
- CONTACT FOR REAGENT AND RESOURCE SHARING
- METHOD DETAILS
    - General Method for the Synthesis of 2-alkoxycarbonyl-*N*-oxide Derivatives
    - Synthesis of 2-Carbamoyl-7-nitro-5-(trifluoromethyl)benzothiazole 3-oxide, Compound 4

- Synthesis of 4-Fluoro-2,6-dinitrophenyl 4-methylbenzenesulfonate, Precursor for Compound 5
- Synthesis of 2-Carbamoyl-5-fluoro-7-nitrobenzothiazole 3-oxide, Compound 5
- Synthesis of 2-Carbamoyl-5-iodo-7-nitrobenzothiazole 3-oxide, Compound 6
- Synthesis of 2-carbamoyl-5-(methoxycarbonyl)-7-nitrobenzothiazole 3-oxide, Compound 7
- Synthesis of 2-Carbamoyl-5-cyano-7-nitrobenzothiazole 3-oxide, Compound 8
- Synthesis of 2-Carbamoyl-5-methyl-7-nitrobenzothiazole 3-oxide , Compound 9
- Synthesis of 2-Carbamoyl-7-nitro-5-((trifluoromethyl)thio)benzothiazole 3-oxide, Compound 10
- Synthesis of 2-Carbamoyl-5-carboxy-7-nitrobenzothiazole 3-oxide, Compound 11
- Synthesis of 2-Cyano-7-nitro-5-(trifluoromethyl)benzothiazole 3-oxide , Compound 12
- Synthesis of 2-(Hydroxycarbamoyl)-7-nitro-5-(trifluoromethyl)benzothiazole 3-oxide , Compound 13
- Synthesis of 2-Carbamoyl-7-nitro-5-(trifluoromethyl)benzothiazole , Compound 14
- Synthesis of 2-Carbamoyl-5-nitro-7-(trifluoromethyl)benzothiazole 3-oxide , Compound 15
- Synthesis of 2-(Hydrazinecarbonyl)-7-nitro-5-(trifluoromethyl)benzothiazole 3-oxide , Compound 16
- Expression and Purification of Plk1 for Kinase Assays
- Construction, Expression and Purification of Cdc25C
- Procedure for PLK1 Assay
- Cloning and Expression of PLK1 C67S
- Procedure for PLK1 and PLK1 C67S Kinase Assay
- Procedures for Molecular Modeling

- QUANTIFICATION AND STATISTICAL ANALYSIS
- DATA AND SOFTWARE AVAILABILITY

SUPPLEMENTAL INFORMATION

Supplemental Information includes six figures and two tables and can be found with this article online.

ACKNOWLEDGMENTS

We would like to thank many at Cyclacel who contributed to this project and also especially acknowledge the Scottish Executive for provision of funding through a SCORE award. We also acknowledge Drs Christopher Meades, Janice McLachlan, Andrew Osnowski, Andy Plater, Joshua Bolger, and James Bozard for their assistance with compound synthesis and BPS Biosciences for the cloning, expression of PLK1 C67S.

AUTHOR CONTRIBUTIONS

R.J.P. synthesized and characterized the molecules used in this study and contributed to the writing of the paper. D.B. was involved in project management and scientific direction. M.M. performed the in vitro kinase assays. P.M.F. was involved in project management and scientific direction. N.J.W. supervised the synthetic chemistry aspects of the study. C.McI. performed the molecular modeling studies, was involved in project management and also contributed extensively to the writing of the paper.

DECLARATION OF INTERESTS

Dr. D. Blake is an employee of Cyclacel, and a shareholder of Cyclacel Pharmaceuticals. Dr. McInnes, as well as an employee of the University of South Carolina, is Founder, President and Chief Scientific Officer of PPI Pharmaceuticals; however, this company was not involved with this published study. Drs. McInnes, Mezna, and Fischer are co-inventors of a patent covering the benzothiazole *N*-oxides described in this study (WO, 2004/05,700 A1).

REFERENCES

Alexandru, G., Uhlmann, F., Mechtler, K., Poupart, M.-A., and Nasmyth, K. (2001). Phosphorylation of the cohesin subunit Scc1 by Polo/Cdc5 kinase regulates sister chromatid separation in yeast. Cell 105, 459–472.

Baillie, T.A. (2016). Targeted covalent inhibitors for drug design. Angew. Chem. Int. Ed. 55, 13408–13421.

Bunting, J.W. (1979). Heterocyclic Meisenheimer complexes. Adv. Heterocycl. Chem. 25, 67–74.

Cohen, M.S., Zhang, C., Shokat, K.M., and Taunton, J. (2005). Structural bioinformatics-based design of selective, irreversible kinase inhibitors. Science 308, 1318–1321.

Craig, S.N., Wyatt, M.D., and McInnes, C. (2014). Current assessment of polo-like kinases as anti-tumor drug targets. Expert Opin. Drug Discov. 9, 773–789.

de Carcer, G., Escobar, B., Higuero, A.M., Garcia, L., Anson, A., Perez, G., Mollejo, M., Manning, G., Melendez, B., Abad-Rodriguez, J., et al. (2011). Plk5, a polo box domain-only protein with specific roles in neuron differentiation and glioblastoma suppression. Mol. Cell. Biol. 31, 1225–1239.

Dohner, H., Lubbert, M., Fiedler, W., Fouillard, L., Haaland, A., Brandwein, J.M., Lepretre, S., Reman, O., Turlure, P., Ottmann, O.G., et al. (2014). Randomized, phase 2 trial comparing low-dose cytarabine with or without volasertib in AML patients not suitable for intensive induction therapy. Blood 124, 1426–1433.

Elez, R., Piiper, A., Giannini, C.D., Brendel, M., and Zeuzem, S. (2000). Polo-like kinase 1, a new target for antisense tumor therapy. Biochem. Biophys. Res. Commun. 269, 352–356.

Elez, R., Piiper, A., Kronenberger, B., Kock, M., Brendel, M., Hermann, E., Pliquett, U., Neumann, E., and Zeuzem, S. (2003). Tumor regression by combination antisense therapy against Plk1 and Bcl-2. Oncogene 22, 69–80.

Elia, A.E., Cantley, L.C., and Yaffe, M.B. (2003a). Proteomic screen finds pSer/pThr-binding domain localizing Plk1 to mitotic substrates. Science 299, 1228–1231.

Elia, A.E., Rellos, P., Haire, L.F., Chao, J.W., Ivins, F.J., Hoepker, K., Mohammad, D., Cantley, L.C., Smerdon, S.J., and Yaffe, M.B. (2003b). The molecular basis for

phosphodependent substrate targeting and regulation of Plks by the Polo-box domain. Cell 115, 83–95.

Feng, P., Lee, K.N., Lee, J.W., Zhan, C., and Ngai, M.Y. (2016). Access to a new class of synthetic building blocks via trifluoromethoxylation of pyridines and pyrimidines. Chem. Sci. 7, 424–429.

Gjertsen, B.T., and Schoffski, P. (2014). Discovery and development of the Polo-like kinase inhibitor volasertib in cancer therapy. Leukemia 29, 11.

Glover, D.M., Hagan, I.M., and Tavares, A.A. (1998). Polo-like kinases: a team that plays throughout mitosis. Genes Dev. 12, 3777–3787.

Golan, A., Yudkovsky, Y., and Hershko, A. (2002). The cyclin-ubiquitin ligase activity of cyclosome/APC is jointly activated by protein kinases Cdk1-cyclin B and Plk. J. Biol. Chem. 277, 15552–15557.

Hamanaka, R., Smith, M.R., O'Connor, P.M., Maloid, S., Mihalic, K., Spivak, J.L., Longo, D.L., and Ferris, D.K. (1995). Polo-like kinase is a cell cycle-regulated kinase activated during mitosis. J. Biol. Chem. 270, 21086–21091.

Jang, Y.-J., Lin, C.-Y., Ma, S., and Erikson, R.L. (2002). Functional studies on the role of the C-terminal domain of mammalian polo-like kinase. Proc. Natl. Acad. Sci. USA 99, 1984–1989.

Kloss, F., Krchnak, V., Krchnakova, A., Schieferdecker, S., Dreisbach, J., Krone, V., Mollmann, U., Hoelscher, M., and Miller, M.J. (2017). In vivo dearomatization of the potent antituberculosis agent BTZ043 via Meisenheimer complex formation. Angew. Chem. Int. Ed. 56, 2187–2191.

Knecht, R., Elez, R., Oechler, M., Solbach, C., Von Ilberg, C., and Strebhardt, K. (1999). Prognostic significance of polo-like kinase (PLK) expression in squamous cell carcinomas of the head and neck. Cancer Res. 59, 2794–2797.

Kotani, S., Tugendreich, S., Fujii, M., Jorgensen, P.M., Watanabe, N., Hoog, C., Hieter, P., and Todokoro, K. (1998). PKA and MPF-activated polo-like kinase regulate anaphase-promoting complex activity and mitosis progression. Mol. Cell 1, 371–380.

Lee, K.S., Grenfell, T.Z., Yarm, F.R., and Erikson, R.L. (1998). Mutation of the polo-box disrupts localization and mitotic functions of the mammalian polo kinase Plk. Proc. Natl. Acad. Sci. USA 95, 9301–9306.

Lee, K.S., Yuan, Y.-L.O., Kuriyama, R., and Erikson, R.L. (1995). Plk is an M-phase-specific protein kinase and interacts with a kinesin-like protein, CHO1/MKLP-1. Mol. Cell. Biol. 15, 7143–7151.

Leung, G.C., Hudson, J.W., Kozarova, A., Davidson, A., Dennis, J.W., and Sicheri, F. (2002). The Sak polo-box comprises a structural domain sufficient for mitotic subcellular localization. Nat. Struct. Biol. 9, 719–724.

McInnes, C., Mazumdar, A., Mezna, M., Meades, C., Midgley, C., Scaerou, F., Carpenter, L., Mackenzie, M., Taylor, P., Walkinshaw, M., et al. (2006). Inhibitors of Polo-like kinase reveal roles in spindle-pole maintenance. Nat. Chem. Biol. 2, 608–617.

McInnes, C., and Wyatt, M.D. (2011). PLK1 as an oncology target: current status and future potential. Drug Discov. Today 16, 619–625.

Nurse, P. (1990). Universal control mechanism regulating onset of M-phase. Nature 344, 503–508.

Roshak, A.K., Capper, E.A., Imburgia, C., Fornwald, J., Scott, G., and Marshall, L.A. (2000). The human polo-like kinase, PLK, regulates cdc2/cyclin B through phosphorylation and activation of the cdc25C phosphatase. Cell. Signal. 12, 405–411.

Seong, Y.-S., Kamijo, K., Lee, J.-S., Fernandez, E., Kuriyama, R., Miki, T., and Lee, K.S. (2002). A spindle checkpoint arrest and a cytokinesis failure by the dominant-negative polo-box domain of Plk1 in U-2 OS cells. J. Biol. Chem. 277, 32282–32293.

Singh, J., Dobrusin, E.M., Fry, D.W., Haske, T., Whitty, A., and McNamara, D.J. (1997). Structure-based design of a potent, selective, and irreversible inhibitor of the catalytic domain of the erbB receptor subfamily of protein tyrosine kinases. J. Med. Chem. 40, 1130–1135.

Smith, M.R., Wilson, M.L., Hamanaka, R., Chase, D., Kung, H., Longo, D.L., and Ferris, D.K. (1997). Malignant transformation of mammalian cells initiated by constitutive expression of the polo-like kinase. Biochem. Biophys. Res. Commun. 234, 397–405.

Spankuch-Schmitt, B., Bereiter-Hahn, J., Kaufmann, M., and Strebhardt, K. (2002a). Effect of RNA silencing of polo-like kinase-1 (PLK1) on apoptosis and spindle formation in human cancer cells. J. Natl. Cancer Inst. 94, 1863–1877.

Spankuch-Schmitt, B., Wolf, G., Solbach, C., Loibl, S., Knecht, R., Stegmuller, M., von Minckwitz, G., Kaufmann, M., and Strebhardt, K. (2002b). Downregulation of human polo-

like kinase activity by antisense oligonucleotides induces growth inhibition in cancer cells. Oncogene 21, 3162–3171.

Sumara, I., Gimenez-Abian, J.F., Gerlich, D., Hirota, T., Kraft, C., de la Torre, C., Ellenberg, J., and Peters, J.M. (2004). Roles of polo-like kinase 1 in the assembly of functional mitotic spindles. Curr. Biol. 14, 1712–1722.

Takahashi, T., Sano, B., Nagata, T., Kato, H., Sugiyama, Y., Kunieda, K., Kimura, M., Okano, Y., and Saji, S. (2003). Polo-like kinase 1 (PLK1) is overexpressed in primary colorectal cancers. Cancer Sci. 94, 148–152.

Taylor, P., Blackburn, E., Sheng, Y.G., Harding, S., Hsin, K.Y., Kan, D., Shave, S., and Walkinshaw, M.D. (2008). Ligand discovery and virtual screening using the program LIDAEUS. Br. J. Pharmacol. 153 (Suppl 1), S55–S67.

Taylor, R. (1970). Novel Meisenheimer complexes, alkyl-2,4,6-trinitrocyclohexadienate anions. J. Org. Chem. 35, 3578–3579.

Tokumitsu, Y., Mori, M., Tanaka, S., Akazawa, K., Nakano, S., and Niho, Y. (1999). Prognostic significance of polo-like kinase expression in esophageal carcinoma. Int. J. Oncol. 15, 687–692.

Toyoshima-Morimoto, F., Taniguchi, E., and Nishida, E. (2002). Plk1 promotes nuclear translocation of human Cdc25C during prophase. EMBO Rep. 3, 341–348.

Wagner, K., Heitzer, H., and Oehlmann, L. (1973). Benzthiazol-N-oxide, I. Synthese und Reaktivitat von 2-Alkoxycarbonyl-benzthiazol-N-oxiden. Chem. Ber. 106, 640–654.

Wagner, K., and Oehlmann, L. (1976). Benzothiazol-N-oxide, IV1) Synthese und Reaktivitat von 2-Cyanbenzothiazol-N-Oxiden und 2-Benzothiazolcarbonitrilen. Chem. Ber. 109, 611–618.

Wolf, G., Elez, R., Doermer, A., Holtrich, U., Ackermann, H., Stutte, H.J., Altmannsberger, H.-M., Rubsamen-Waigmann, H., and Strebhardt, K. (1997). Prognostic significance of polo-like kinase (PLK) expression in nonsmall cell lung cancer. Oncogene 14, 543–549.

Wu, S.Y., McNae, I., Kontopidis, G., McClue, S.J., McInnes, C., Stewart, K.J., Wang, S., Zheleva, D.I., Marriage, H., Lane, D.P., et al. (2003). Discovery of a novel family of CDK inhibitors with the program LIDAEUS: structural basis for ligand-induced disordering of the activation loop. Structure 11, 399–410.

Yuan, J., Hoerlin, A., Hock, B., Stutte, H.J., Ruebsamen-Waigmann, H., and Strebhardt, K. (1997). Polo-like kinase, a novel marker for cellular proliferation. Am. J. Pathol. 150, 1165–1172.

Yuan, J., Sanhaji, M., Kramer, A., Reindl, W., Hofmann, M., Kreis, N.N., Zimmer, B., Berg, T., and Strebhardt, K. (2011). Polo-box domain inhibitor poloxin activates the spindle assembly checkpoint and inhibits tumor growth in vivo. Am. J. Pathol. 179, 2091–2099.

Zhao, Z., Liu, Q., Bliven, S., Xie, L., and Bourne, P.E. (2017). Determining cysteines available for covalent inhibition across the human kinome. J. Med. Chem. 60, 2879–2889.

STAR METHODS

KEY RESOURCES TABLE

REAGENT or RESOURCE	SOURCE	IDENTIFIER
Chemicals, Peptides, and Recombinant Proteins		
Triethylamine	Sigma-Aldrich	T0886
Ethyl thioglycolate	Sigma-Aldrich	E34307
Ammonium hydroxide solutions	Sigma-Aldrich	338818
2-Chloro-5-trifluoromethyl-1,3-dinitrobenzene	TCI Europe	C0994
4-Fluoro-2,6-dinitrophenol	Fisher Scientific	11403557
2-Chloro-5-iodo-1,3-dinitrobenzene	ACES Phamra, Inc.	112587
2-Chloro-5-methoxycarbonyl-1,3-dinitrobenzene	Carbosynth Ltd	FM67720
2-Chloro-5-cyano-1,3-dinitrobenzene	Carbosynth Ltd	FC70294
2-Chloro-5-methyl-1,3-dinitrobenzene	Sigma-Aldrich	PH011654
2-Chloro-5-(trifluoromethylthio)-1,3-dinitrobenzene	NONE	Can be synthesized according to: Journal of Fluorine Chemistry, 125(9), 1305-1316; 2004
Sodium hydroxide	Sigma-Aldrich	795429
Phosphorus oxychloride	Sigma-Aldrich	262099
Pyridine	Sigma-Aldrich	270970
Hydroxylamine solution	Sigma-Aldrich	467804
Triethylphosphine	Sigma-Aldrich	245275

2-Chloro-1,5-dinitro-3-(trifluoromethyl)benzene	CambridgeChem	318514052
Hydrazine solution	Sigma-Aldrich	751855
Sf9 cells in Sf-900^{TM} II SFM	ThermoFisher	11496015
Plk1 open reading frame (X75932)	Clontech	HA040548
BL21(DE3)pLysS Chemically Competent E. coli	ThermoFisher	C606003
Critical Commercial Assay		
PLK1 Kinase Assay	BPS Bioscineces LLC	PLK1
Software and Algorithms		
Insight II	Biovia	Affinity
PyMol	Schrodinger	https://pymol.org/2/

CONTACT FOR REAGENT AND RESOURCE SHARING

Further information and requests for resources and reagents should be directed to and will be fulfilled by the Lead Contact, Campbell McInnes (mcinnes@cop.sc.edu).

METHOD DETAILS

General Method for the Synthesis of 2-alkoxycarbonyl-*N*-oxide Derivatives

See Figure S5 for synthetic scheme (McInnes et al., 2006). Step 1: Triethylamine (1.1 eq) was added to a suspension of 5 substituted, 1,3-dinitrobenzyl-2-chloride (1eq) and ethyl thioglycolate (1 eq) in ethanol (3 cm^3) at 10-20 ^oC (Supplementary Figure 5.). Onset of the reaction was observed by the solvent beginning to reflux even though the mixture was being cooled in a water bath. After stirring for a further 3h a precipitate formed which was collected by filtration, washed with ice-cold water followed by a further wash with ice-cold methanol. Recrystallization from methanol gave the desired ethyl ester derivatives. Step 2: The 2-alkoxycarbonylbenzothiazol-3-oxide (1 eq) was suspended in ethanol (2 cm^3) at 20-30 ^oC and

ammonium hydroxide (1.2 eq) added. After stirring for 4h , the desired 2-carbamoyl benzthiazol-3-oxide crystallised from solution, was collected by filtration and was washed with ice-cold water and then methanol. Recrystallisation from methanol gave the desired amide derivatives. For further information see McInnes et al., 2006.

Synthesis of 2-Carbamoyl-7-nitro-5-(trifluoromethyl)benzothiazole 3-oxide, Compound 4

The general method above was followed using 2-chloro-5-trifluoromethyl-1,3 dinitrobenzene. The title compound was obtained as a yellow crystalline solid: 1H NMR (DMSO-d_6, 500 MHz): δ_H 8.76 (2H, s, Ar-H and NH), 8.96 (1H, s, Ar-H) and 9.36 (1H, s, NH). MS (ESI^+) *m/z* 308.01 $[M+H]^+$ ($C_9H_5N_3O_4F_3S$ requires 308.00). mp 222-223 ^oC (lit 225-226 ^oC, Wagner et al., 1973). Anal. RP-HPLC: t_R 13.75 min. (10-70% MeCN).

Synthesis of 4-Fluoro-2,6-dinitrophenyl 4-methylbenzenesulfonate, Precursor for Compound 5

4-Fluoro-2,6-dinitrophenol (1 eq) was dissolved in toluene (5 cm^3) and tosyl chloride (1.1 eq) added followed by pyridine (1.1 eq) (Figure S6). After stirring for 12 h a white precipitate formed which was collected by filtration. The mother liquor was evaporated to dryness and used without further purification. ^1H NMR (DMSO-d_6, 500 MHz): δ_H 2.48 (3H, s, CH_3), 7.50 (2H, d, *J* 8.0, 2 x Ar-H), 7.67 (2H, d, *J* 8.0, 2 x Ar-H) and 8.51 (2H, d, *J* 8.0, 2 x Ar-H).

Synthesis of 2-Carbamoyl-5-fluoro-7-nitrobenzothiazole 3-oxide, Compound 5

The title compound was obtained as a yellow crystalline solid from 4-fluoro-2,6-dinitrophenyl 4-methylbenzenesulfonate using the general method for the synthesis of 2-alkoxycarbonyl-*N*-oxides. ^1H NMR (DMSO-d_6, 500 MHz): δ_H 8.82 (1H, s, NH), 8.88 (1H, d, *J* 7.5, Ar-H), 8.97 (1H, d, *J* 7.5, Ar-H) and 9.41 (1H, s, NH). $C_8H_5N_3O_4FS$ requires M 257.99848, found 257.99861. mp 282-283 ^oC. Anal. RP-HPLC: t_R 9.83 min. (10-70% MeCN).

Synthesis of 2-Carbamoyl-5-iodo-7-nitrobenzothiazole 3-oxide, Compound 6

The title compound was obtained as a yellow crystalline solid from 2-chloro-5-iodo-1,3 dinitrobenzene using the general method. ^{1}H NMR (DMSO-d_6, 500 MHz): δ_H 8.81 (1H, s, Ar-H), 8.82 (1H, s, NH), 8.94 (1H, s, Ar-H), and 9.41 (1H, s, NH). $C_8H_4N_3O_4IS$ requires *M* 364.89673, found 364.89634.

Synthesis of 2-carbamoyl-5-(methoxycarbonyl)-7-nitrobenzothiazole 3-oxide, Compound 7

The title compound was obtained as a yellow crystalline solid from 2-chloro-5 methoxycarbonyl-1,3-dinitrobenzene using the general method. ^{1}H NMR (DMSO-d_6, 300 MHz): δ_H 3.89 (3H, s, CH_3), 8.78 (4H, s, 2 Ar-H and 2 NH).

Synthesis of 2-Carbamoyl-5-cyano-7-nitrobenzothiazole 3-oxide, Compound 8

The title compound was obtained as a yellow crystalline solid from 2-chloro-5-cyano-1,3-dinitrobenzene using the general method. ^{1}H NMR (DMSO-d_6, 500 MHz): δ_H 8.86 (1H, s, NH), 9.16 (1H, s, Ar-H), 9.22 (1H, s, Ar-H) and 9.33 (1H, s, NH). $C_9H_4N_4O_4S$ requires *M* 263.9953, found 263.9951. mp 222-223 ^{o}C (lit 225-226 ^{o}C, Wagner and Oehlmann., 1976), Anal. RP-HPLC: t_R 19.60 min. (10-70% MeCN).

Synthesis of 2-Carbamoyl-5-methyl-7-nitrobenzothiazole 3-oxide , Compound 9

The title compound was obtained as a yellow crystalline solid from 2-chloro-5-methyl-1,3-dinitrobenzene using the general method. mp 271-272 ^{o}C (lit 274-275 ^{o}C, Wagner et al., 1973). Anal. RP-HPLC: t_R 11.32 min. (10-70% MeCN).

Synthesis of 2-Carbamoyl-7-nitro-5-((trifluoromethyl)thio)benzothiazole 3-oxide, Compound 10

The title compound was obtained as a yellow crystalline solid from 2-chloro-5-(trifluoromethylthio)-1,3-dinitrobenzene using the general method. ^{1}H NMR (DMSO-d_6, 500 MHz): δ_H 8.82 (1H, s, Ar-H), 8.85 (1H, s, Ar-H), 8.90 (1H, s, NH) and 9.35 (1H, s, NH). $C_9H_5N_3O_4F_3S_2$ requires *M* 339.96736, found 339.96739. mp 255-256 ^{o}C, Anal. RP-HPLC: t_R 15.79 min. (10-70% MeCN).

Synthesis of 2-Carbamoyl-5-carboxy-7-nitrobenzothiazole 3-oxide, Compound 11

Compound **7** (26 mg, 0.09 mmol) was suspended in water (1.0 ml) containing methanol (0.1 ml). Sodium hydroxide (4 mg, 0.1 mmol) in water (0.36 ml) was added and the resultant precipitate collected by filtration and washed with water. The title compound was obtained as a yellow crystalline solid, ^{1}H NMR (DMSO-d_6, 500 MHz): δ_H 7.88 (1H, s, Ar-H) and 8.35 (1H, s, Ar-H), $C_9H_5N_3O_6S$ requires *M* 282.9899, found 282.9900. mp 181-183 ^{o}C (lit 188-190 ^{o}C, Wagner et al., 1973), t_R 16.38 min. (10-70% MeCN).

Synthesis of 2-Cyano-7-nitro-5-(trifluoromethyl)benzothiazole 3-oxide , Compound 12

Phosphorus oxychloride (306 mg, 0.186 ml, 2.0 mmol) was added to a suspension of **4** (672 mg, 2.0 mmol) in dry pyridine (1 ml) at 20-30 ^{o}C and stirred for 12 h (Wagner and Oehlmann., 1976). Ice-water was added and the resultant precipitate collected by filtration. The title compound was obtained as a yellow crystalline solid. ^{1}H NMR (DMSO-d_6, 500 MHz): δ_H 8.91 (1H, s, Ar-H) and 9.02 (1H, s, Ar-H). mp 188-189 ^{o}C (lit 190-191 ^{o}C, Wagner et al., 1973), t_R 15.60 min. (10-70% MeCN).

Synthesis of 2-(Hydroxycarbamoyl)-7-nitro-5-(trifluoromethyl)benzothiazole 3-oxide , Compound 13

The title compound was obtained as a yellow crystalline solid from the reaction of compound **4** with hydroxylamine using routine methodology (Wagner et al., 1973). ^{1}H NMR (DMSO-d_6, 500 MHz): δ_H 8.86 (1H, s, Ar-H), 8.96 (1H, s, Ar-H), 10.17 and 12.13 (2H, s, NH and OH). MS (ESI$^+$) *m/z* 346.00 $[M+Na]^+$ and 324.07 $[M+H]^+$ ($C_9H_4N_3O_5F_3S$ requires 322.98). mp 230-231 ^{o}C (lit 234-235 ^{o}C, Wagner et al., 1973). Anal. RP-HPLC: t_R 12.33 min. (10-70% MeCN).

Synthesis of 2-Carbamoyl-7-nitro-5-(trifluoromethyl)benzothiazole , Compound 14

Compound **4** (30 mg, 0.097 mmol) was dissolved in ethanol (2 ml) and heated to 70 ^{o}C. Triethyl phosphine (17 mg, 1.1 eq) was added and the mixture remained at 70 ^{o}C for a further 4 h. On cooling the resultant precipitate was collected by filtration. The title compound was

obtained as a yellow crystalline solid: ^{1}H NMR (DMSO-d_6, 500 MHz): δ_H 8.36 (1H, s, NH), 8.68 (1H, s, NH), 8.77 (1H, s, Ar-H) and 8.92 (1H, s, Ar-H). mp 222-224 ^{o}C (lit 225-226 ^{o}C, Wagner and Oehlmann., 1976). Anal. RP-HPLC: t_R 16.01 min. (10-70% MeCN).

Synthesis of 2-Carbamoyl-5-nitro-7-(trifluoromethyl)benzothiazole 3-oxide , Compound 15

The title compound was obtained as a yellow crystalline solid from 2-chloro-1,5-dinitro-3-(trifluoromethyl)benzene using the general method. ^{1}H NMR (DMSO-d_6, 500 MHz): δ_H 8.88 (1H, s, Ar-H), 8.90 (1H, s, NH), 8.97 (1H, s, Ar-H) and 9.33 (1H, s, NH), $C_9H_4F_3N_3O_4S$ requires *M* 306.9875, found 306.9880. mp 224-225 ^{o}C (lit 225-226 ^{o}C, Wagner et al., 1973).

Synthesis of 2-(Hydrazinecarbonyl)-7-nitro-5-(trifluoromethyl)benzothiazole 3-oxide , Compound 16

The title compound was obtained as a yellow crystalline solid from the reaction of compound **4** with hydrazine using standard procedures (Wagner et al., 1973). ^{1}H NMR (DMSO-d_6, 500 MHz): δ_H 5.20 (2H, s, NH_2), 8.88 (1H, s, Ar-H), 8.95 (1H, s, Ar-H) and 11.20 (1H, s, NH). mp 229-230 ^{o}C (lit 232-233 ^{o}C, Wagner et al., 1973). Anal. RP-HPLC: t_R 11.88 min. (10-70% MeCN).

Expression and Purification of Plk1 for Kinase Assays

The Plk1 open reading frame (X75932) was amplified from a fetal lung complementary DNA library (Clontech) using primers incorporating restriction enzyme sites. The 50 primer (5'-GCCGCTAGCGACGATGACGATAAGATGAGTGCTGCAGTGACTGCAGGGAAGC-3') had an NheI site upstream of the ATG start codon. The 3' primer (5'-GGAATTCTTAGGAGGCCTTGAGACGG-3') incorporated an EcoRI site downstream of the stop codon. The PCR product was subcloned into the NheI/EcoRI sites of a baculovirus expression vector (pSSP1) derived from pFastBac Hta (Invitrogen). Cloning into this vector resulted in a hexahistidine-tag fusion at the N terminus of the Plk1 construct. Sf9 strain cells of a passage number less than 20 were split back to give a 300-ml culture volume, at a cell density of 1.5 3 106 cells ml_1. Cells were only used for expression in logarithmic growth phase. Plk1 baculovirus (from P2 amplification) was added to give a multiplicity of infection

of 3; this is equivalent to three virus particles for each insect cell. The flasks were incubated at 27 °C, with shaking at 100 r.p.m., for 48 h. On harvest, cell density and viability were determined, and the cultures were spun down at 2,500 r.p.m. for 5 min and washed with ice-cold (0 °C) phosphate-buffered saline. The wash was re-spun at the same speed and the pellet was snap frozen. Plk1 protein was purified on a metal affinity column. The insect cell pellet was lysed in a buffer (10 mM Tris-HCl, pH 8.0, 150 mM NaCl, 5 mM β-mercaptoethanol, 1 mM PMSF, 1 mM benzamidine, 20 mM imidazole and protease inhibitor cocktail (Sigma)) and the precleared supernatant was loaded onto Ni-NTA-agarose (Qiagen). The affinity column was washed with the lysis buffer and the bound protein was eluted with 250 mM imidazole in the same buffer. After overnight dialysis against 25 mM Tris-HCl, pH 7.5, 100 mM NaCl, 1 mM DTT, 1 mM PMSF, 1 mM benzamidine, protease inhibitor cocktail (Sigma) and 10% glycerol, the purified protein was stored at -70 °C until used.

Construction, Expression and Purification of Cdc25C

Using standard techniques a full-length Cdc25C clone was isolated by PCR from HeLa mRNA and inserted on a BamHI-HindIII fragment into the plasmid pRsetA. The N-terminal Cdc25C fragment (encoding residues 1–300) was excised from this vector and inserted into the plasmid pET28a (between the NcoI and BamHI sites). Expression was under the control of the T7 promoter, and the encoded protein contains a hexahistidine tag at the C terminus. The vector was transformed into E. coli strain BRL(DE3) pLysS for expression experiments. The protein was expressed in BL21(DE3) RIL bacteria cells that were grown in LB medium at 37 °C until optical density at 600 nm of 0.6 was reached. Expression was induced with 1 mM IPTG, and the bacterial culture was grown further for 3 h. The bacteria were harvested by centrifugation and the cell pellet resuspended in 50 mM Tris, pH 7.5, and 10% sucrose, flash frozen, and stored at -70 °C until used. Purification of the protein was then carried out by lysing the bacterial pellet in 10 ml of lysis buffer (10 mM Tris-HCl, pH 8.0, 150 mM NaCl, 5 mM β-mercaptoethanol and 20 mM imidazole) supplemented with a cocktail of protease inhibitors and sonicated six times at 20-s bursts. The lysate was then centrifuged for 15 min at 15,000 r.p.m. and filtered through a 0.45-mm filter. The sample was then loaded onto a Ni-NTA agarose column and washed several times, and then the Cdc25 protein was eluted with a buffer containing 10 mM Tris-HCl, pH 8.0, 100 mM NaCl, 5 mM β-mercaptoethanol, 0.02% Nonidet P-40 (EMD Millipore) and 250 mM imidazole. The eluate

was then dialyzed, concentrated, snap frozen in liquid nitrogen and stored at -70 ^{o}C until used.

Procedure for PLK1 Assay

PLK1 kinase activity (compounds in Tables 1 and 2) was assayed using either Casein or the N-terminal domain of the human Cdc25C phosphatase (a natural substrate for PLK1) as substrates. The assays were carried out using a 96-well plate format by incubating Cdc25C (2 mg/well) or Casein (50 mg/well) with varying concentrations of the Ni-NTA purified PLK1 and varying concentrations of the negative, non-transformed host Sf9 cell lysate in a total volume of 25 ul of 20 mM Tris/HCl buffer pH 7.0, supplemented with 25 mM β-glycerophosphate, 5 mM EGTA, 1 mM DTT and 1 mM $NaVO_3$. Reaction was initiated by the addition of 100 mM ATP and 0.5 mCi of [γ-^{32}P]-ATP. The reaction mixture was incubated at 30 ^{o}C for 1 h, then stopped with 75 mM aq orthophosphoric acid, transferred onto a 96-well P81 filter plate (Whatman), dried, and the extent of Cdc25C phosphorylation was assessed by scintillation counting using a Packard TopCount plate reader.

Cloning and Expression of PLK1 C67S

This was undertaken at BPS Bioscience (San Diego). After C67S mutation and C-terminal His tag were introduced by PCR, the insert was cloned into pFastBac vector (Thermo Fisher Scientific), followed by sequence analysis. The plasmid was transformed into DH10Bac^{TM}. E. coli Competent Cells (Thermo Fisher Scientific) where it recombined with the parent bacmid to form an expression bacmid. The purified bacmid DNA was tested for recombination by PCR. Then the bacmid DNA was transfected into insect cells for production of recombinant baculovirus particles. P3 virus was used for protein production. Protein was expressed in Sf9 cells using recombinant baculovirus at a MOI of 3 grown in SF900II media (Gibco_). Cell were harvest by centrifugation three days after transfection and His tagged protein was purified using Ni-NTA affinity. Briefly, cells were lysed by sonication after resuspension in TBS-T buffer. Protein was purified using Ni^{2+}-NTA agarose (Sigma) eluting with TBS-T buffer plus imidazole. High purity elutions as assessed by SDS PAGE were pooled with glycerol and DTT added to a final concentration of 20% and 3 mM respectively. Protein was quantified by Bradford reagent (Pierce^{TM}) using BSA as the standard. Purity was determined to be >90% by SDS PAGE.

Procedure for PLK1 and PLK1 C67S Kinase Assay

For the data shown in Figures 5 and S3, the assay was performed by BPS Bioscience (San Diego) using Kinase-Glo Plus luminescence kinase assay kit (obtained from Promega). It measures kinase activity by quantitating the amount of ATP remaining in solution following a kinase reaction. The luminescent signal from the assay is correlated with the amount of ATP present and is inversely correlated with the amount of kinase activity. The compounds were diluted in 10% DMSO and 5ml of the dilution was added to a 50 ml reaction so that the final concentration of DMSO is 1% in all of reactions. All of the enzymatic reactions were conducted at 30 ^{o}C for 45 minutes for the wild type PLK1 and 60 min for PLK1(C67S). The 50 ml reaction mixture contains 40 mM Tris, pH 7.4, 10 mM $MgCl_2$, 0.1 mg/ml BSA, 1 mM DTT, 0.1 mg/ml PLK1 peptide substrate, 10 mM (or 5 mM) ATP and PLK1. After the enzymatic reaction, 50 ml of Kinase-Glo Plus Luminescence kinase assay solution (Promega) was added to each reaction and incubate the plate for 15 minutes at room temperature. The luminescence signal was measured using a BioTek Synergy 2 microplate reader.

Procedures for Molecular Modeling

The homology model for PLK1 was generated using the program module Homology within the molecular modelling package InsightII (Accelrys, San Diego, CA) using PKA as a template structure. Compounds were docked with the PLK1 homology model using the Affinity program within InsightII implementing a molecular dynamics docking routine. The binding site was defined as an 8 Å radius from the centre of a ligand placed in the ATP site. The calculation was performed using the CVFF force field in a two-step process and an implicitly derived solvation model and geometric H-bond restraints. Initially, the inhibitor was minimized into the ATP cleft, using a simple non-bonded method where the Coulombic and Van der Waals terms are scaled to zero and 0.1, respectively. The refinement phase involved molecular dynamics calculated over 5 ps in 100 fs stages, where the temperature was scaled from 500 K to 300 K followed by a final minimisation over 1,000 steps using the Polak-Ribiere Conjugate Gradient method. The docked structures were ranked energetically using the in-house developed programs Calsor and Calsorcont and the Ludi module of InsightII.

QUANTIFICATION AND STATISTICAL ANALYSIS

PLK1 activity assays were performed in duplicate at each concentration. The luminescence data were analyzed using the computer software, Graphpad Prism. The difference between luminescence intensities in the absence of PLK1 (Lut) and in the presence of PLK1 (Luc) was defined as 100 % activity (Lut – Luc). Using luminescence signal (Lu) in the presence of the compound, % activity was calculated as:

% activity = {(Lut - Lu)/(Lut - Luc)} x 100%, where Lu= the luminescence intensity in the presence of the compound (all percent activities below zero were shown zero in the table).

The values of % activity versus a series of compound concentrations were then plotted using non-linear regression analysis of Sigmoidal dose-response curve generated with the equation Y=B+(T-B)/1+10((LogEC50-X)xHill Slope), where Y=percent activity, B=minimum percent activity, T=maximum percent activity, X= logarithm of compound and Hill Slope=slope factor or Hill coefficient. The IC50 value was determined by the concentration causing a half-maximal percent activity.

DATA AND SOFTWARE AVAILABILITY

No data or software beyond what is included in this manuscript and supplementary information are available.

Table 1. Structure-Activity Relationships for the Benzothiazole *N*-Oxide PLK1 Inhibitors

Compound	Structure				Kinase Inhibition (μM)	
	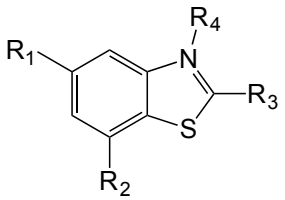					
	R_1	R_2	R_3	R_4	PLK1	CDK2/Cyclin E
4	CF_3	NO_2	$CONH_2$	O	2.47 ± 1.23	> 100
5	F	NO_2	$CONH_2$	O	18.1 ± 2.69	> 100
6	I	NO_2	$CONH_2$	O	0.36 ± 0.01	> 100
7	$COOCH_3$	NO_2	$CONH_2$	O	7.11 ± 0.86	> 100
8	CN	NO_2	$CONH_2$	O	8.4 ± 0.86	44.2 ± 3.18
9	CH_3	NO_2	$CONH_2$	O	> 100	> 100
10	SCF_3	NO_2	$CONH_2$	O	0.39 ± 0.07	> 100
11	COOH	NO_2	$CONH_2$	O	> 100	
12	CF_3	NO_2	CN	O	17.0 ± 4.24	
13	CF_3	NO_2	CONHOH	O	31.0 ± 15.6	> 100
14	CF_3	NO_2	$CONH_2$	-	> 100	
15	NO_2	CF_3	$CONH_2$	O	> 100	
16	CF_3	NO_2	$CONHNH_2$	O	> 100	

Table 2. Spectroscopic Results of Benzothiazole *N*-Oxide Meisenheimer Formation (in the Presence of *n*-BuNH$_2$)

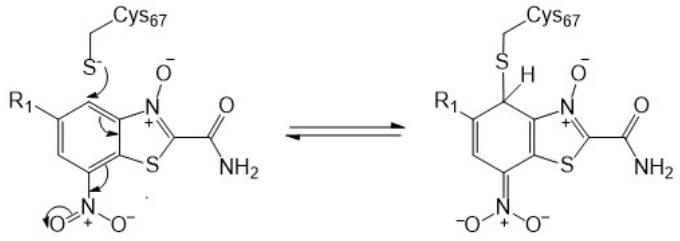

R_1 = CF_3, SCF_3, CN, CO_2CH_3, I

Compound[a]	R1	PLK1 IC_{50} (μM) When R_3 = $CONH_2$	δ_{Ar1} (ppm)[b]	δ_{Ar2} (ppm)[b]	δ_{Ar1} (ppm)[b] + *n*-$BuNH_2$	δ_{Ar2} (ppm)[b] + *n*-$BuNH_2$	λ_{max} (nm), ε (L mol^{-1} cm^{-1})[c]	λ_{max} (nm), ε (L mol^{-1} cm^{-1})[c] + *n*-$BuNH_2$
4a	CF_3	2.47 ± 1.23	9.00-8.99	8.85-8.84	6.78-6.77	6.61	405, 5,369	440, 24,832
5a	F	18.1 ± 2.69	-	-	-	-	380, 3,143	450, 7,924
6a	I	0.36 ± 0.01	8.94	8.81	-	-	410, 3,937	465, 12,992
7a	$COOCH_3$	7.11 ± 0.86	8.96	8.81	7.10	-7.00	400, 2,443	420, 19,870
8a	CN	8.4 ± 0.86	-	-	-	-	410, 4,399	450, 14,076
9a	CH_3	> 100	8.65	8.42	8.70-8.40	8.70-8.40	400, 5,085	395, 5,367
10a	SCF_3	0.39 ± 0.07	8.93	8.78	6.78	6.64	405, 4,412	445, 18,382
11a	COOH	> 100	8.96	8.80	9.00	8.82	395, 4,063	390, 4,375

Position C4 of the benzothiazole N-oxide is less hindered, favored by the SNAr mechanism and in close proximity to C67 in the docked models.

[a]Primary amide of R3 is replaced by COOEt.

[b]All ^{1}H NMR performed in $CDCl_3$.

[c]All UV-vis in EtOH.

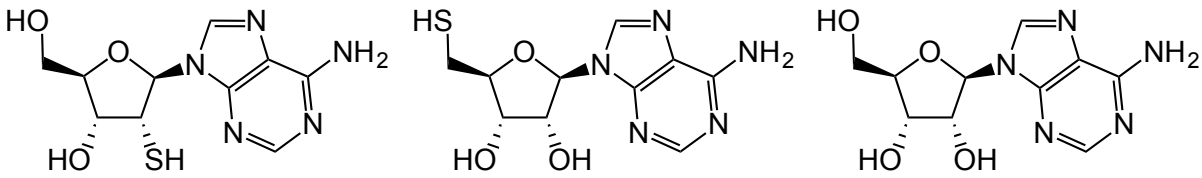

1 **2** **3**

Figure 1. Chemical Structures of PLK1 Inhibitory Compounds (2TA, **1**; 5TA, **2**; and adenosine **3**) Used in Validation of the Homology Model and for Probing the Covalent Modification of the ATP Binding Site

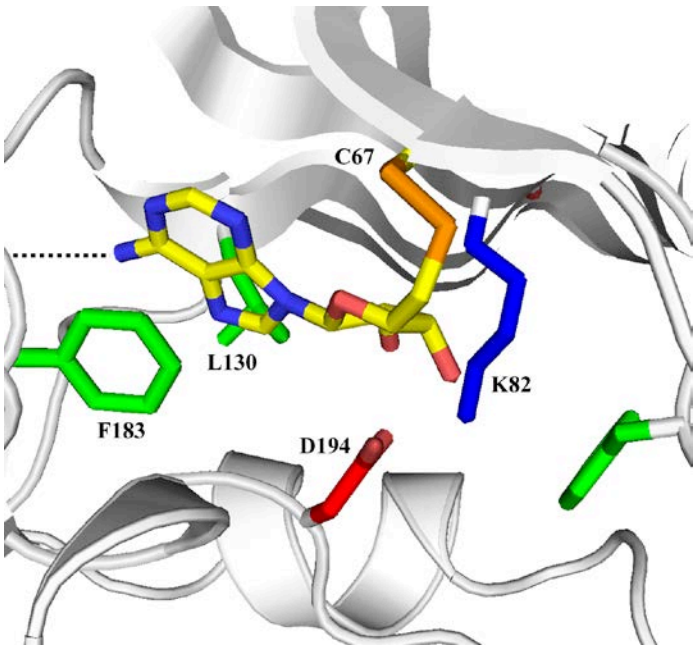

Figure 2. Complex of 5TA, 2, with the ATP Binding Site of PLK1

Complex was generated through flexible docking of the free thiol compound into the PLK1 homology model with selected conformations that correspond to the known binding mode of ATP derivatives. The irreversible inhibition of this derivative is supported by the formation of the disulfide linkage in silico and minimization of the covalently linked inhibitor.

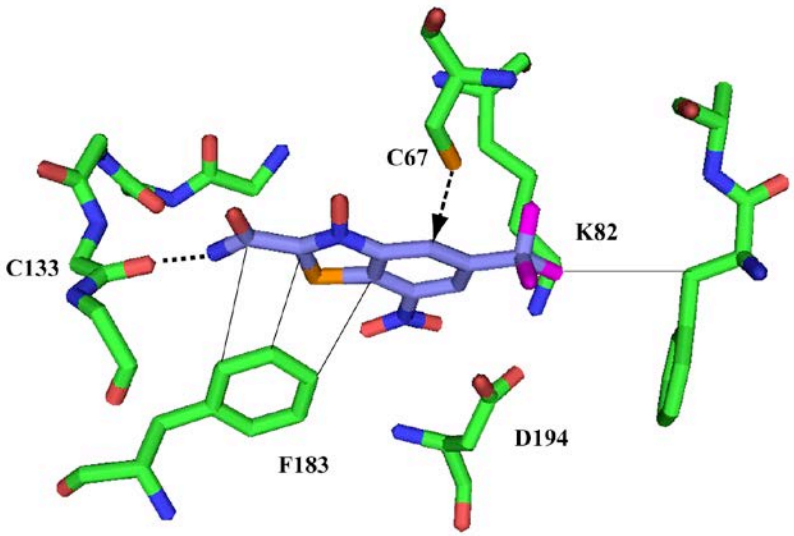

Figure 3. Molecular Docking of the *In-Silico*-Discovered Benzothiazole *N*-Oxide, 4, with the ATP Binding Site of PLK1

The binding mode was predicted based on most favorable interaction energies and the SAR of the primary amide group is thus consistent with hinge H-bonding interactions. The displayed pose is consistent with the Meisenheimer hypothesis requiring the proximity of the benzothiazole C4 to the attacking thiol nucleophile from C67.

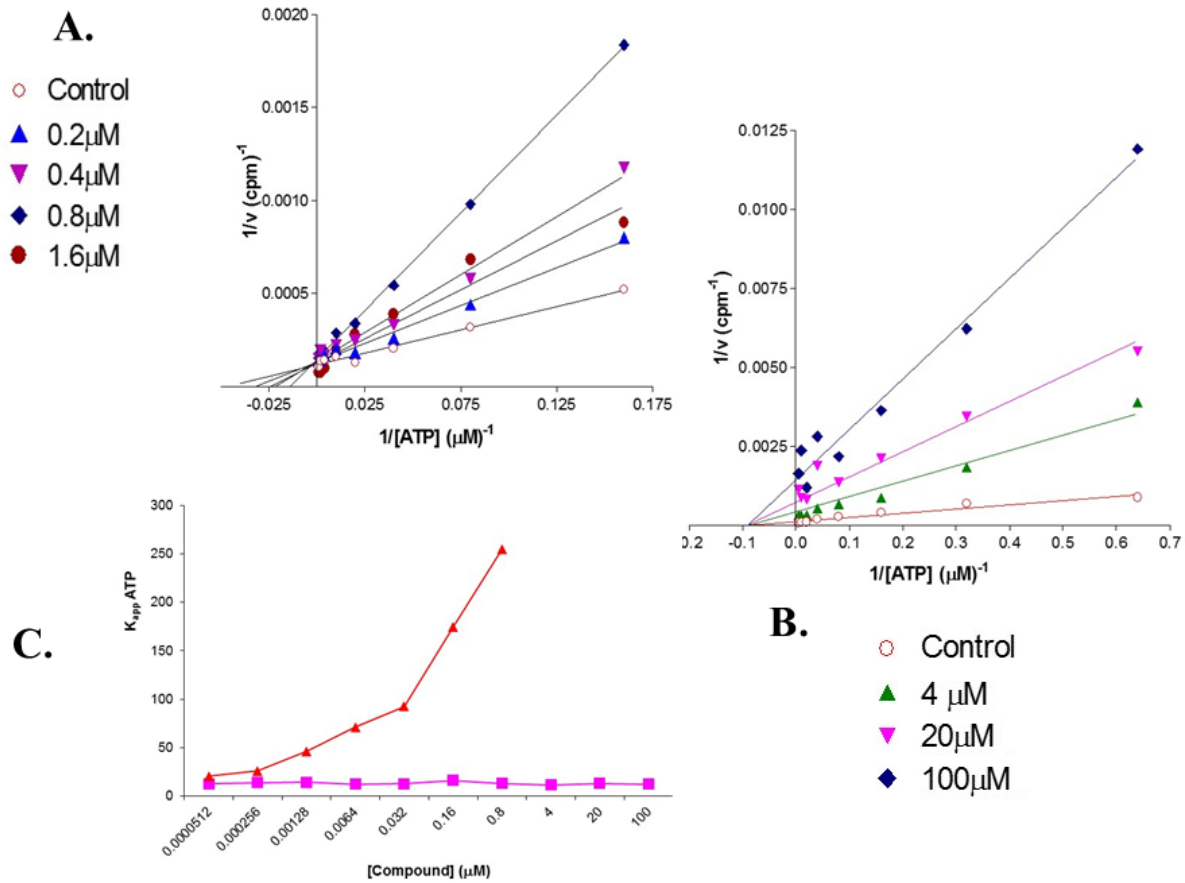

Figure 4. Enzyme Kinetics of Benzothiazole *N*-Oxide PLK1 Inhibitors

(A and B) Lineweaver Burk Plot analysis of compounds **4** and **10** suggest that they act via competitive (A) and non-competitive (B) binding, respectively. (C) The ATP dependence of these two inhibitors further confirms this analysis (compound **4** with red data points and **10** in magenta).

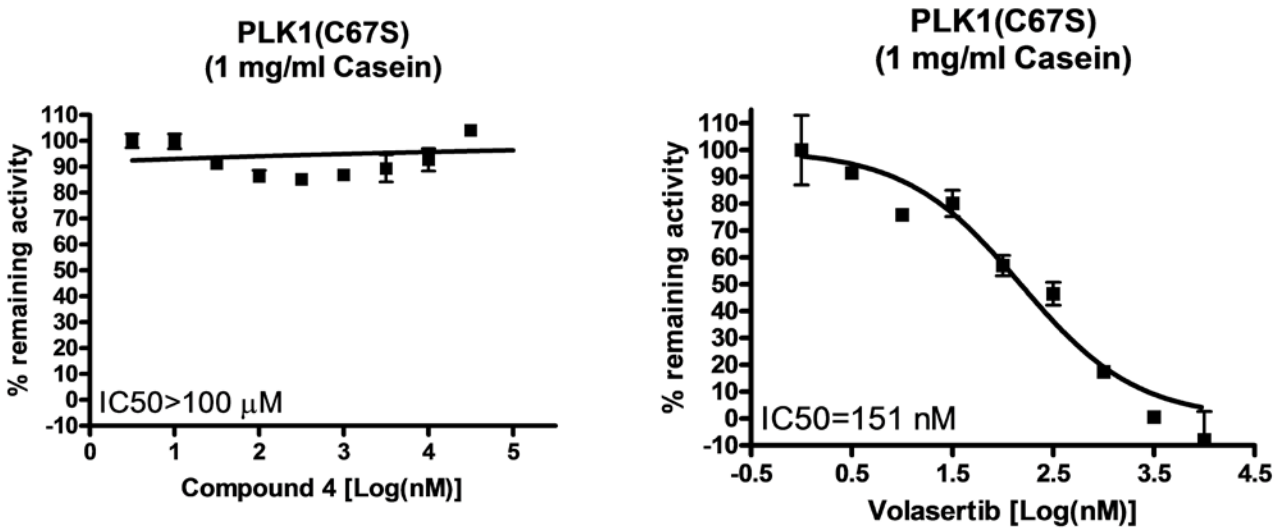

Figure 5. Comparison of the Activities of Compound 4 (left) and volasertib (right) against PLK1 C67S, a Mutant Designed to Test the Contributions to C^{67} to the Activity of the Benzothiazole *N*-Oxide Series (error bars represent standard deviations calculated for duplicate experiments).

The data obtained for the replacement of the cysteine with a serine, an isosteric residue, and which is considerably less nucleophilic, confirms the formation of the Meisenheimer complex with **4**.

Graphical Abstract

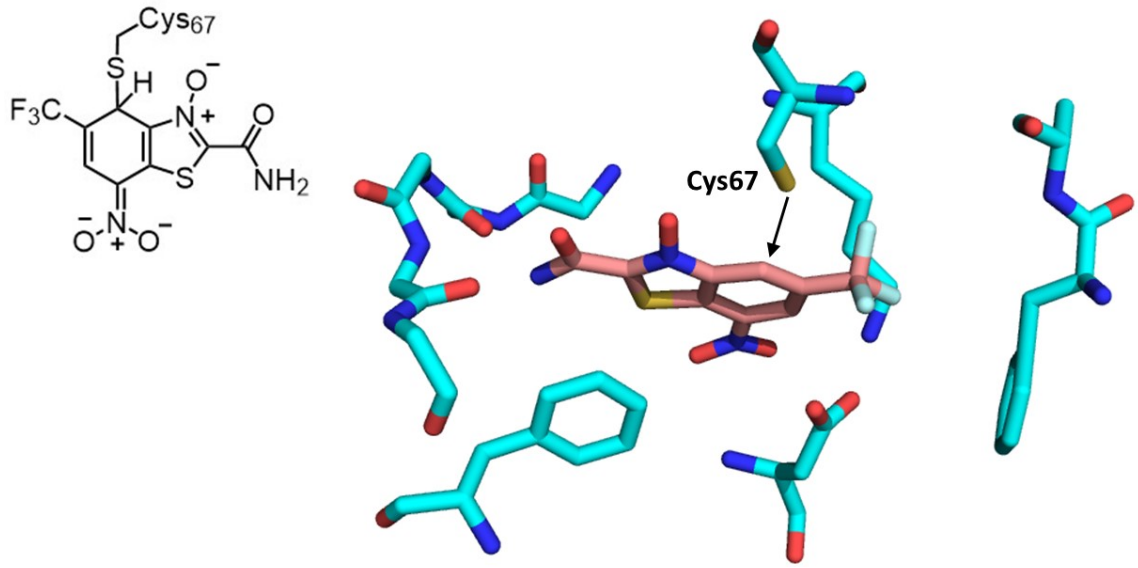

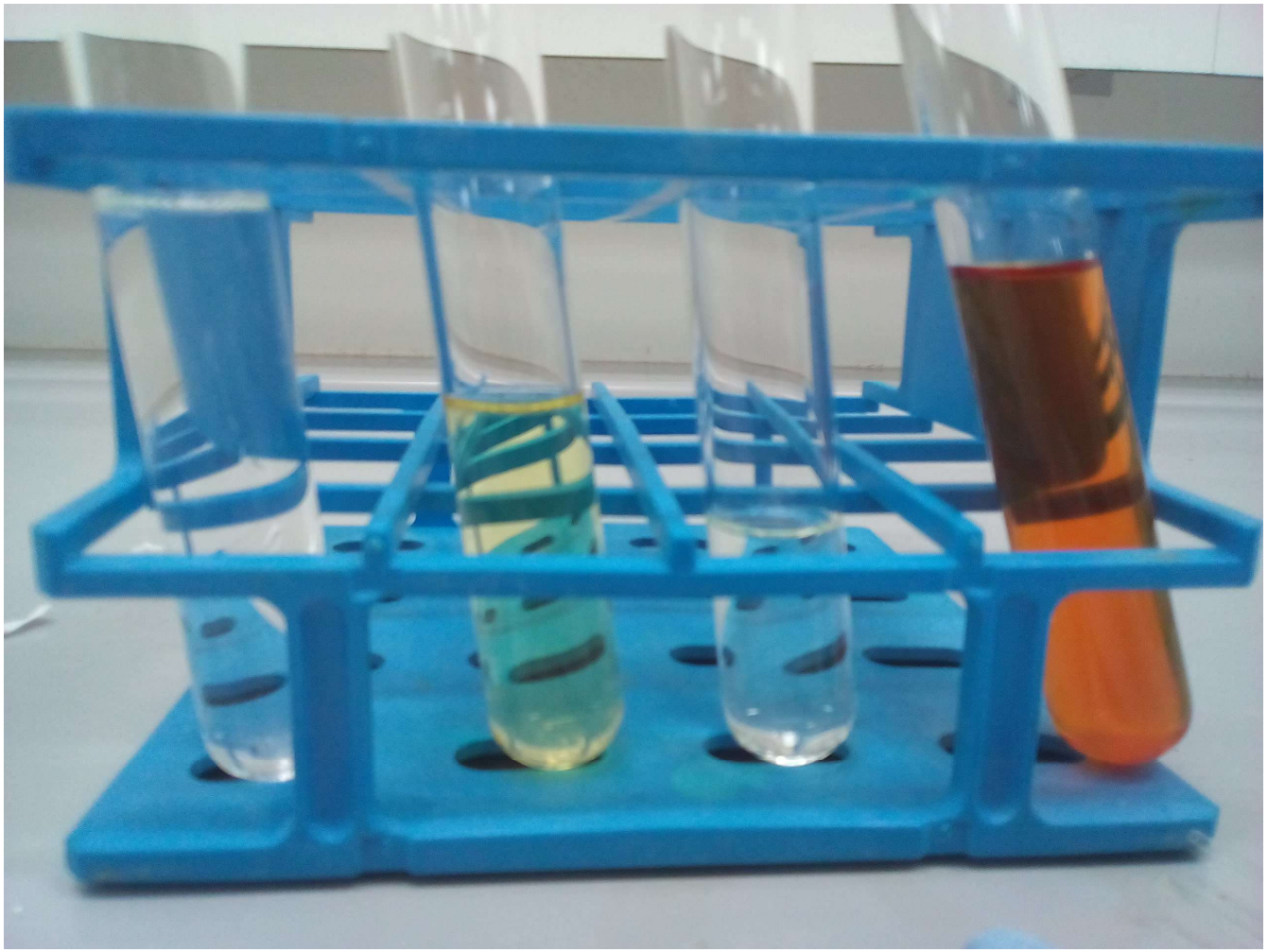

Far left is the blank (so EtOH)

Second left is compound 10 (concentration 1.18x10-3M) in EtOH.

Second right is compound 10 (after 10 fold dilution, so 1.18x10-4M) in EtOH

Far right is compound 10 (concentration 1.18x10-3M) + 9eq sodium 1-butanethiolate in EtOH

SUPPLEMENTARY FIGURE 1 (related to Table 2). UV Evidence for Meisenheimer complex with a thiolate nucleophile.

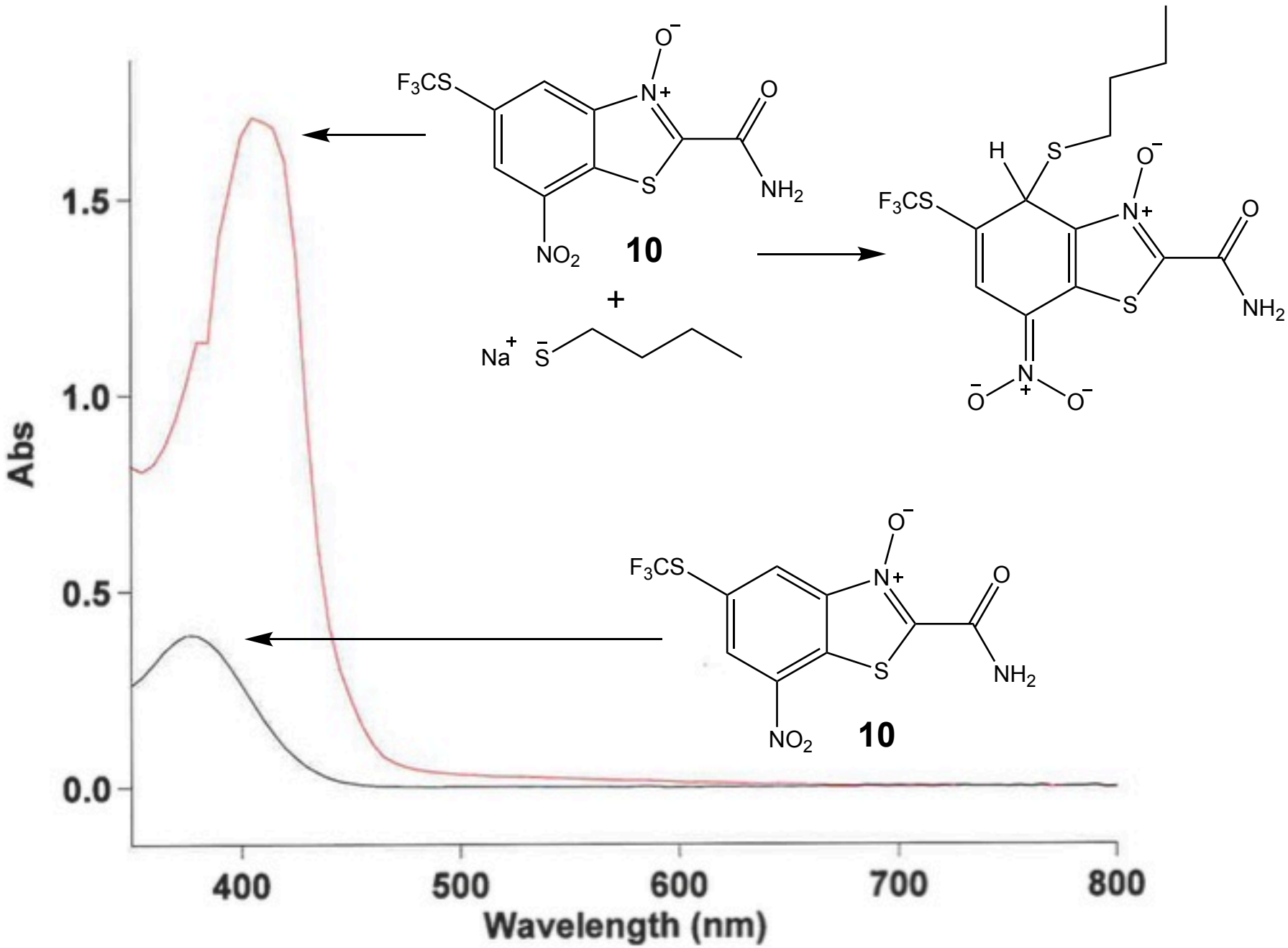

SUPPLEMENTARY FIGURE 2 (Related to Table 2) UV Trace of addition of sodium n-butylthiolate to compound 10

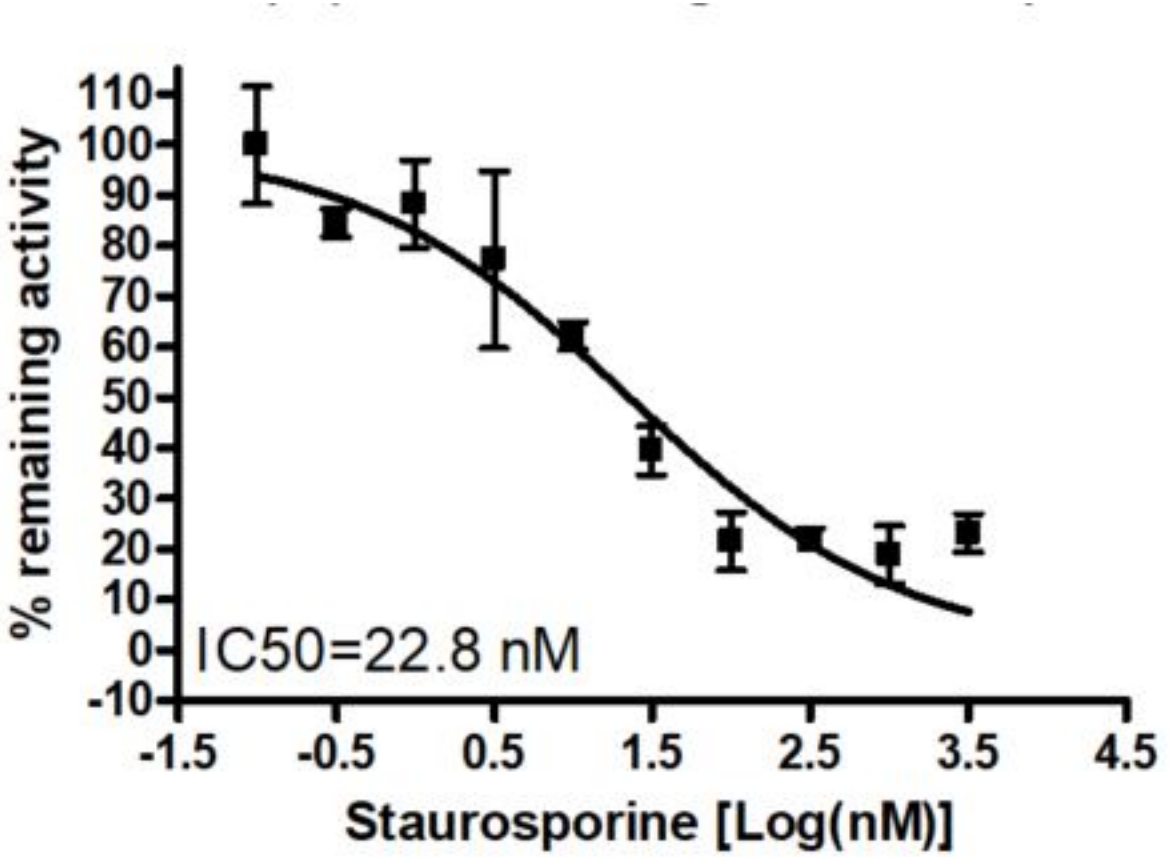

Supplementary Figure 3 (Related to Figure 5). Dose-reponse curve for the inhibition of PLK1 C67S with staurosporine and showing that potent inhibition is retained.

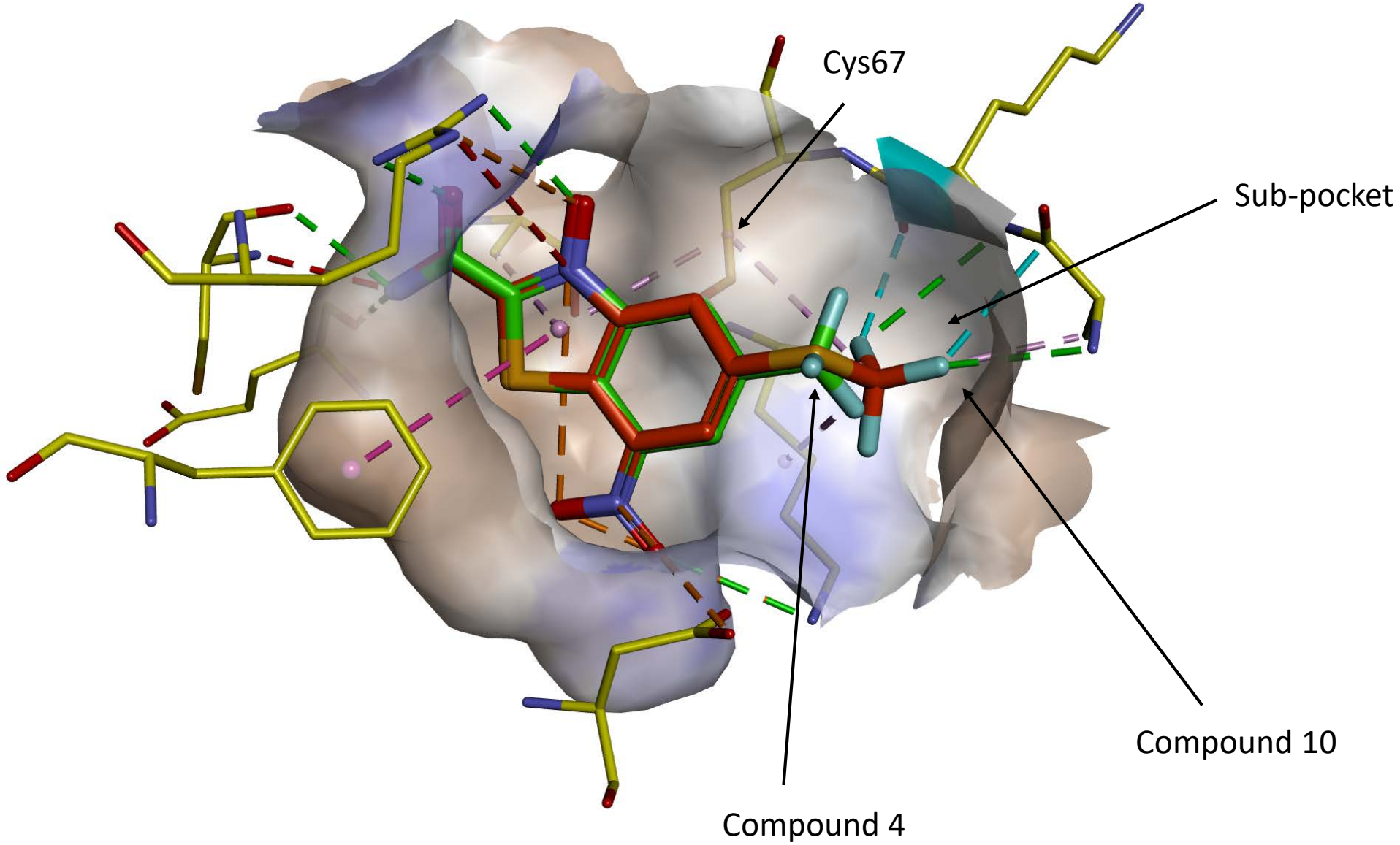

Supplementary Figure 4 (Related to Table 1 and Figure 3). Binding mode of compounds **4** and **10** showing covalent interaction with Cys67. The additional interactions of the SCF_3 group in **10** are highlighted.

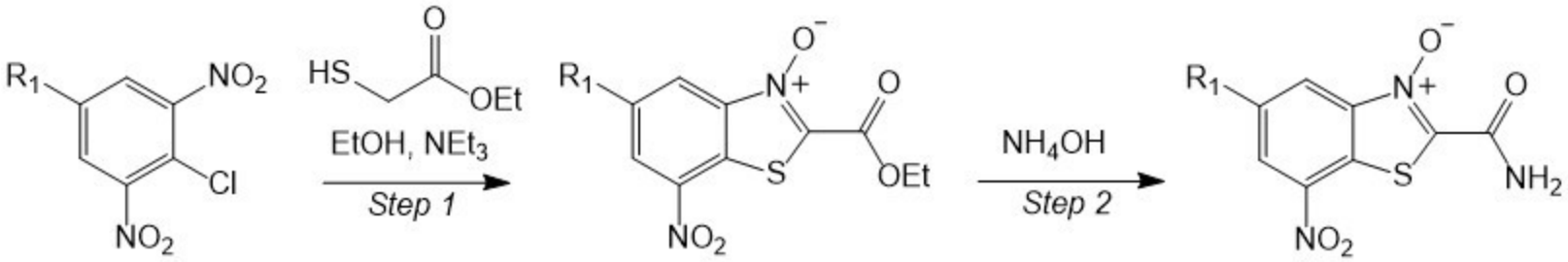

Supplementary Figure 5. (related to Table1) - Synthetic Scheme for benzthiazole N-oxides

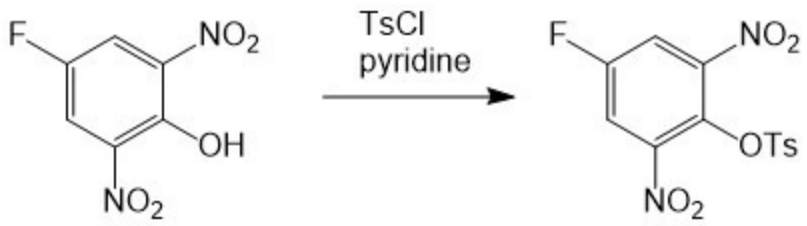

Supplementary Figure 6 (Related to Table1) Synthesis of Precursor for compound 5.

Kinase	benzthiazole 4	benzthiazole 10
Plk1	2.47	0.39
Cdk2/E	>100	>100
Cdk2/A	>100	>100
Cdk1/B	>100	>100
Cdk4/D1	>100	>100
Cdk7/H	>100	>100
Cdk9/T	>100	>100
CK II	>100	>100
CamK II	>100	>100
MAPK2/ERK	>100	>100
PKC a	>100	>100
Akt/PKB	>100	>100
Abl	>100	>100
GSK3a	>100	>100
Aurora A	>100	>100
PKA	>100	>100
P70S6K	>100	>100
SAPK2	>100	>100

Further testing of compound 8 on an additional panel of 20 kinases extented the selectivity

Supplementary table 1 (Related to Table 1) Kinase Selectivity of Benzthiazoles 4 and 10 relating to Results section entitled “Kinase Selectivity and Cellular activity of lead inhibitors”

Enzyme	Activity (% of control)
c-RAF	108 ± 10
CDK2/E	88 ± 4
Chk1	111 ± 7
Chk2	97 ± 10
CSK	45 ± 2
FGFR3	83 ± 10
IGF-1R	98 ± 6
IKKα	115 ± 14
IR	107±12
JNK2α2	10 6± 1
MAPKAP-K2	96 ± 11
MEK1	96 ± 6
MKK6	88 ± 5
MSK1	106 ± 5
PDGFRα	108 ± 8
PKCγ	117 ± 15
PKCβII	82 ± 14
Rsk2	105 ± 5
SAPK2b	94 ± 3
SAPK3	120 ± 6
Yes	108 ± 12

Supplementary Table 2. (Related to Table 1) Screening of compound **4** against a panel of 21 kinases from the Millipore Sigma. The percent inhibition of each enzyme is reported at 100 μM compound. This table related to Results section entitled "Kinase Selectivity and Cellular activity of lead inhibitors"